Mena binds α5 integrin directly and modulates α5β1 function

Stephanie L. Gupton,[1,2] Daisy Riquelme,[1,2] Shannon K. Hughes-Alford,[1,2,3] Jenny Tadros,[1,2] Shireen S. Rudina,[3] Richard O.Hynes,[1,2,4] Douglas Lauffenburger,[1,2,3] and Frank B. Gertler[1,2]

[1]The David H. Koch Institute for Integrative Cancer Research, [2]Department of Biology, and [3]Department of Biological Engineering, Massachusetts Institute of Technology, Cambridge, MA 02139
[4]Howard Hughes Medical Institute, Chevy Chase, MD 20815

Mena is an Ena/VASP family actin regulator with roles in cell migration, chemotaxis, cell–cell adhesion, tumor cell invasion, and metastasis. Although enriched in focal adhesions, Mena has no established function within these structures. We find that Mena forms an adhesion-regulated complex with α5β1 integrin, a fibronectin receptor involved in cell adhesion, motility, fibronectin fibrillogenesis, signaling, and growth factor receptor trafficking. Mena bound directly to the carboxy-terminal portion of the α5 cytoplasmic tail via a 91-residue region containing 13 five-residue "LERER" repeats. In fibroblasts, the Mena–α5 complex was required for "outside-in" α5β1 functions, including normal phosphorylation of FAK and paxillin and formation of fibrillar adhesions. It also supported fibrillogenesis and cell spreading and controlled cell migration speed. Thus, fibroblasts require Mena for multiple α5β1-dependent processes involving bidirectional interactions between the extracellular matrix and cytoplasmic focal adhesion proteins.

Introduction

The ECM is a mesh of proteins secreted, assembled, and remodeled dynamically by cells that contact it (Wickström et al., 2011; Hynes and Naba, 2012). Fibroblasts are a major source of ECM proteins and regulate ECM homeostasis in tissues and organs (McAnulty, 2007). Cell migration and differentiation are among many processes controlled by the ECM as it engages adhesion receptors and presents matrix-bound growth factors to cell surface receptors. The ECM protein fibronectin (FN) is a ubiquitous component of the interstitial matrix (Singh et al., 2010). Outside the bloodstream, cells typically assemble soluble FN dimers into complex meshworks of fibrils (Schwarzbauer and DeSimone, 2011), which provide a supporting scaffold that delivers multivalent, spatially organized biochemical and mechanical signals that influence cell behavior (Hynes, 2009; Huttenlocher and Horwitz, 2011; Geiger and Yamada, 2011).

The predominant ECM receptors are integrins, a family of heterodimeric transmembrane proteins composed of α and β subunits that link the ECM to the cytoskeleton and transmit signals and mechanical forces bidirectionally across the plasma membrane (Hynes, 2002). Integrins are regulated by clustering and conformational changes triggered either by binding to ECM ligands or by interaction between the intracellular tails of integrin subunits and cytoplasmic proteins (Margadant et al., 2011). The β subunit cytoplasmic tails share significant sequence similarity; several cytoplasmic proteins directly bind most β subunits to regulate integrin activation, trafficking, and signaling (Calderwood, 2004; Moser et al., 2009). In contrast, α integrin subunit tails share a short, conserved membrane-proximal sequence that interacts directly with the β subunit, with proteins that regulate integrin trafficking (Ivaska and Heino, 2011), and with Sharpin, a negative regulator of integrin activation (Rantala et al., 2011). Less is known about the potential unique functions conferred by the distal, divergent cytoplasmic tails of the 18 α subunits.

Correspondence to Stephanie L. Gupton: stephanie_gupton@med.unc.edu; or Frank Gertler: fgertler@mit.edu

Stephanie L. Gupton's present address is Dept. of Cell and Developmental Biology, University of North Carolina at Chapel Hill, Chapel Hill, NC 27599.

Abbreviations used in this paper: CDM, cell-derived matrix; ES, embryonic stem; FA, focal adhesion; FB, fibrillar adhesion; FN, fibronectin; FP4, FPPPP; FX, focal complex; pFAK, phosphor-FAK; pPax, phosphor-paxillin; pY, phosphotyrosine; RIAM, Rap1-GTP–interacting adaptor molecule; VASP, vasodilator-stimulated phosphoprotein.

The Rockefeller University Press $30.00
J. Cell Biol. Vol. 198 No. 4 657–676
www.jcb.org/cgi/doi/10.1083/jcb.201202079

αVβ3 and α5β1 are the two major FN receptors (Hynes, 2002). α5β1 is the primary receptor for soluble FN and has a key role in assembling FN into fibrils, though αVβ3 can assemble fibrils in cells that lack α5β1 (Yang et al., 1999). Typically, however, the two receptors exert distinct effects on cell motility, invasion, signaling, and matrix remodeling (Clark et al., 2005; Caswell et al., 2008, 2009; Wickström et al., 2011).

Integrin-based ECM adhesions are complex structures that turn over continually and change their composition and morphology (Geiger and Yamada, 2011). New adhesions form as small integrin-rich punctae at the cell periphery; associated cytoplasmic proteins bound to integrin tails recruit additional signaling, adaptor, or actin-binding proteins (Vicente-Manzanares and Horwitz, 2011). Nascent adhesions enlarge into transient focal complexes (FXs) that mature into focal adhesions (FAs), elongated structures of variable size and composition that are connected to the distal ends of F-actin bundles. In some cell types, including fibroblasts, α5β1 exits FAs, moves toward the cell interior along stress fibers (Pankov et al., 2000), and forms stable fibrillar adhesions (FBs) that mediate FN fibrillogenesis. FBs are enriched for FN, α5β1, and tensin (which is absent from FXs and found only weakly in FAs; Pankov et al., 2000; Zamir et al., 2000; Zaidel-Bar et al., 2007). FBs lack components found in FAs, including phosphotyrosine (pY)-containing proteins, vinculin, FAK, and zyxin. α5β1 drives fibrillogenesis by translocating bound FN out of FAs to FBs: the movement generates contractile forces on the α5β1 connection between the cytoskeleton and FN, causing conformational changes in both α5β1 and FN; these changes strengthen and prolong binding (Margadant et al., 2011) and expose self-association sites that align nascent FN fibrils with intracellular actin bundles (Schwarzbauer and DeSimone, 2011).

Ena/vasodilator-stimulated phosphoprotein (VASP) actin-regulatory proteins have diverse roles in cell movement and morphogenesis (Drees and Gertler, 2008; Bear and Gertler, 2009; Homem and Peifer, 2009): they promote formation of longer, less-branched F-actin networks and increase F-actin elongation rates by transferring actin monomer from profilin to free barbed ends while protecting growing filaments from capping proteins that terminate polymerization (Bear and Gertler, 2009; Dominguez, 2009; Hansen and Mullins, 2010). Ena/VASP proteins are concentrated at the tips of lamellipodia and filopodia (sites of rapid actin assembly), and localize prominently to cell–cell and cell–matrix adhesions; they interact with several FA components, including vinculin, zyxin, Rap1-GTP–interacting adaptor molecule (RIAM), and palladin (Pula and Krause, 2008). The function of Ena/VASP in FAs is not well understood, but they regulate integrin activation. For example, VASP negatively regulates αIIbβ3 activation (Aszódi et al., 1999; Hauser et al., 1999).

The three vertebrate Ena/VASP proteins Mena, VASP, and EVL share conserved domains (Gertler et al., 1996), including: (a) an N-terminal EVH1 domain that binds to proteins that typically contain one or more EVH1-binding sites with an optimal core consensus motif of "FPPPP" (FP4; Ball et al., 2002); however, unconventional EVH1 ligands have been identified (Boëda et al., 2007). (b) A proline-rich center, containing binding sites for SH3 and WW domains and for profilin (which binds actin monomers; Ferron et al., 2007). (c) A C-terminal EVH2 domain that contains G and F-actin binding sites and a coiled-coil that mediates their tetramerization (see Fig. 3 A; Zimmermann et al., 2002; Barzik et al., 2005). Each of the three proteins can support many Ena/VASP-dependent cellular functions such as filopodial protrusion (Applewhite et al., 2007; Dent et al., 2007), formation of functional endothelial barriers (Furman et al., 2007), or stimulation of actin-based motility of the intracellular pathogen *Listeria monocytogenes* (Geese et al., 2002). However, Mena contains the "LERER repeat," a unique region of unknown function, with 13 repeats of a 5-residue motif within a 91-residue span between the EVH1 domain and proline-rich core (Gertler et al., 1996).

We found that the LERER repeat interacts with the cytoplasmic tail of α5 integrin, and mediates a robust adhesion-modulated interaction between Mena and α5β1 that contributes to key α5β1 functions: FN fibrillogenesis, cell spreading, motility, and activation of adhesion-dependent signaling. We conclude that Mena is involved in both inside-out and outside-in signaling through α5β1.

Results

Relocalization of Mena to mitochondrial recruits α5

While investigating Ena/VASP- and integrin-mediated neuritogenesis (Gupton and Gertler, 2010), we observed that artificially relocalized Ena/VASP influenced α5β1 subcellular distribution. We depleted Ena/VASP from their normal locations and sequestered them on the mitochondrial surface by expressing a construct containing multiple EVH1-binding sites fused to a mitochondrial-targeting motif (FP4-Mito; Bear et al., 2000). FP4-Mito expression phenocopies defects that arise from loss of Ena/VASP function in fibroblasts, endothelial cells, neurons, and in *Drosophila melanogaster*, where transgenic expression of FP4-Mito phenocopies axon guidance and epithelial defects observed in Ena mutants (Bear et al., 2002; Dent et al., 2007; Furman et al., 2007; Gates et al., 2007). Despite redistribution of Ena/VASP proteins to the mitochondrial surface by FP4-Mito, localization of known Ena/VASP-binding partners such as the FA proteins zyxin and vinculin is unaffected, and no defects are evident when FP4-Mito is expressed in Ena/VASP-deficient cells (Bear et al., 2000).

Primary fibroblasts transfected with GFP-tagged FP4-Mito, and stained with anti-Mena and anti-α5 antibodies, exhibited the expected redistribution of Mena (not depicted); however, α5 integrin, which localizes to the lamellipodium, to small adhesion sites behind the lamellipodium (likely FXs), and to larger FA-like structures (Zamir et al., 2000) in untransfected cells, was unexpectedly recruited to the mitochondrial surface (Fig. 1 A) concurrent with a loss of detectable α5 signal elsewhere in the cell (Fig. 1). This FP4-Mito–dependent α5 relocalization was seen in several fibroblastic cell types, including NIH3T3 and Rat2 cells (Fig. S1 A and not depicted).

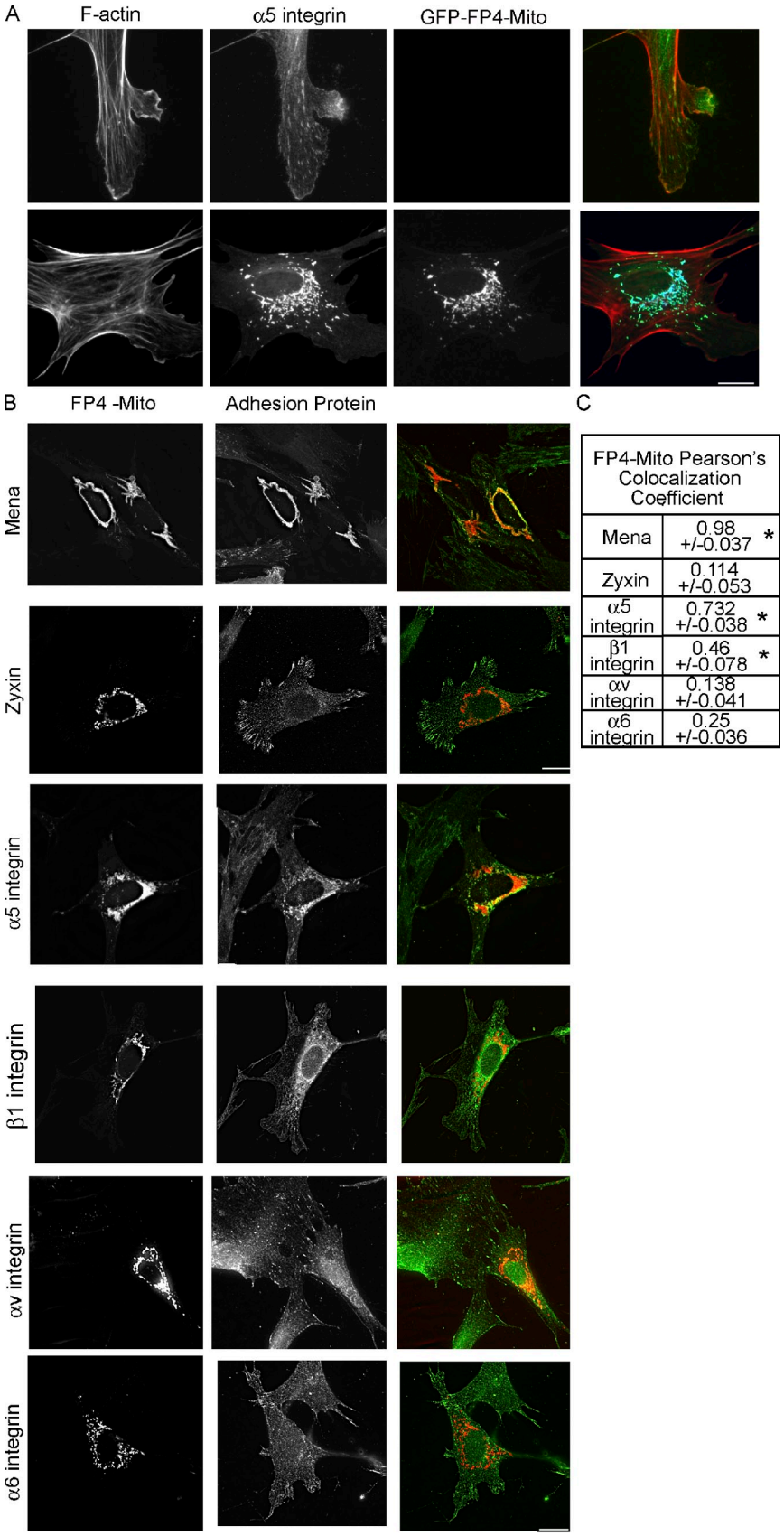

C

FP4-Mito Pearson's Colocalization Coefficient	
Mena	0.98 +/-0.037 *
Zyxin	0.114 +/-0.053
α5 integrin	0.732 +/-0.038 *
β1 integrin	0.46 +/-0.078 *
αv integrin	0.138 +/-0.041
α6 integrin	0.25 +/-0.036

Figure 1. **FP4-Mito recruits α5 integrin to the mitochondrial surface.** (A) Anti-α5 staining in wild-type primary fibroblasts (top) or in cells expressing FP4-Mito (bottom). Phalloidin staining shows F-actin distribution. (B) MV^{D7} cells expressing GFP-Mena transiently transfected with mCherry-FP4-Mito (red) and stained for indicated adhesion component (green). (C) Pearson's coefficients of colocalization of adhesion proteins with FP4-Mito; *, $P < 0.05$ compared with a shuffled image. Bars, 10 μm.

Expression of the control construct "DP4-Mito," which cannot bind Ena/VASP, failed to recruit Ena/VASP proteins to mitochondria, and had no effect on α5 localization (Fig. S1 A). These data were confirmed by Western blot analysis of mitochondria isolated from NIH3T3 cells (Fig. S1 B).

To determine if Ena/VASP could recruit other integrins or FA components to the mitochondrial surface, we used immunostaining of cells expressing FP4-Mito: both Mena and α5 were significantly redistributed to the mitochondrial surface (Fig1, B and C), as was a fraction of the β1 integrin pool (likely by association with α5); however, we saw no significant relocalization of αv- and α6-integrins and zyxin (Fig. 1, B and C). Therefore, Ena/VASP-dependent α5β1 recruitment to mitochondria via FP4-Mito is specific and does not affect other integrins or FA proteins tested.

It is possible that such recruitment to mitochondria occurs by capture of α5β1-containing vesicles by Ena/VASP, in which case the cytoplasmic tails of α5β1 may remain accessible to bind the mitochondrial-tethered Ena/VASP proteins directly or indirectly. To determine whether such vesicle capture occurs during a particular stage of trafficking, FP4-Mito–expressing cells were immunostained for markers of vesicle populations involved in α5β1 trafficking pathways (Caswell et al., 2009; Margadant et al., 2011): EEA1, an early endosomal marker; Rab7, for vesicles containing activated β1 integrins (Arjonen et al., 2012); and Rab11, which decorates α5β1-containing vesicles as they pass through the perinuclear recycling compartment (Margadant et al., 2011). None of the markers were enriched on the α5β1-coated mitochondria of FP4-Mito expressing cells (Fig. S1 D).

We used the FP4-Mito assay to examine the Ena/VASP–α5 integrin interaction in MV^{D7} cells, derived from Mena/VASP double null embryos that express only trace levels of EVL (Bear et al., 2000); expression of FP4-Mito in MV^{D7} cells failed to relocalize α5 to mitochondria (Fig. 2 A), except when GFP-Mena (but not EVL or VASP) was coexpressed (Fig. 2, A and B). To determine if endogenous Mena forms complexes with α5, we immunoprecipitated α5 from NIH3T3 cell lysates followed by Western blot analysis (Fig. 2 C and Fig. S1 C). As expected, β1 was enriched in the immunoprecipitates, as was Mena; however, neither paxillin nor p34 (a component of the Arp2/3 complex) were detected (Fig. 2 C). Therefore, Mena is present in specific complexes with α5 integrin.

The LERER repeat mediates Mena–α5 interaction

We next transfected FP4-Mito into cells that express a series of characterized GFP-tagged Mena deletion mutants, and stained them for α5 to map the regions in Mena (Fig. 3 A) required to interact with α5 (Loureiro et al., 2002). As expected, the GFP-tagged EVH1 domain of Mena was recruited to FP4-Mito–labeled mitochondria, though α5 localization was unaffected (Fig. 3, C and D), which indicates that interaction with α5 requires additional Mena sequences. A mutant lacking the proline-rich region of Mena (MenaΔPro) co-recruited α5 integrin to mitochondria, whereas α5 distribution was unchanged in a mutant lacking the LERER repeat (MenaΔLERER; Fig. 3, C and D); this indicates that the LERER repeat (LERER is the consensus motif repeated within this region; Fig. 3 B), but not Mena's proline-rich central core, is required to recruit α5 to FP4-Mito–labeled mitochondria. GFP-Mena, but not GFP-MenaΔLERER, could be detected in Western blot analysis of α5 immunoprecipitates from MV^{D7} cells that express intact GFP-Mena or GFP-MenaΔLERER (Fig. 3 E). We conclude that the LERER repeat is necessary for complex formation between Mena and α5 integrin.

α5 binds directly to the LERER repeat

Because the LERER repeat is necessary to detect the Mena–α5 complex, we asked whether it is sufficient to mediate the interaction. We expressed a GFP-LERER fusion in MV^{D7} cells that also express mCherry-Mena. GFP-LERER was enriched significantly in peripheral FAs that contain both α5 and mCherry-Mena, but was weak/undetectable in adhesions containing only α5 or mCherry-Mena (Fig. 4, A and E); thus, targeting of GFP-LERER to α5-containing adhesions may arise because of association with the LERER repeat in Mena. The LERER repeat is predicted to form a coiled-coil structure that might dimerize or oligomerize (Fig. S2 E). To test whether intact Mena is required for GFP-LERER to localize to α5-containing adhesions, we next expressed the construct in parental MV^{D7} cells. We found that the GFP-LERER signal is diffuse, with no significant colocalization with α5 (Fig. 4 E), although it was present in some FA-like structures present along F-actin (Fig. 4 A, bottom).

Can the LERER repeat bind directly to the α5 cytoplasmic tail? Like other Ena/VASP proteins, Mena forms stable tetramers through a coiled-coil sequence at the C terminus of the EVH2 domain (Zimmermann et al., 2002; Barzik et al., 2005). Reasoning that tetramerization could affect binding to the α5 tail, we generated constructs to express a His-tagged fusion of the LERER repeat to the Mena EVH2 domain (His-LERER-EVH2) or to the EVH2 domain alone (His-EVH2). Purified His-LERER-EVH2 or His-EVH2 proteins were mixed with purified GST fused to the GST-α5 cytoplasmic tail (GST-α5 tail), or to GST alone, immobilized on glutathione beads (see Coomassie-stained gels of purified proteins in Fig. S2, A–C). After incubation, GST and GST-α5 beads containing bound His-LERER-EVH2 or His-EVH2 were recovered, along with aliquots of unbound protein from the supernatant, and analyzed by Western blotting with anti-His antibodies. His-LERER-EVH2 (Fig. 4 B, top) but not His-EVH2 (Fig. 4 B, bottom) was detected in the fraction bound by GST-α5; neither protein was detected in the GST-bound fraction. When a fusion of the LERER repeat alone to the His tag (His-LERER) was used in the assay, His-LERER was detected in the fraction bound to GST-α5 but not to GST alone (Fig. 4 C). Therefore, the LERER repeat binds directly to the α5 tail.

Next, we delineated sequences within the α5 tail that bind Mena. A GST-α5 tail construct lacking the five C-terminal residues failed to capture His-LERER (Fig. 4 C). We asked whether the free C-terminal end of the α5 tail is required to bind Mena by expressing a full-length α5 expression construct

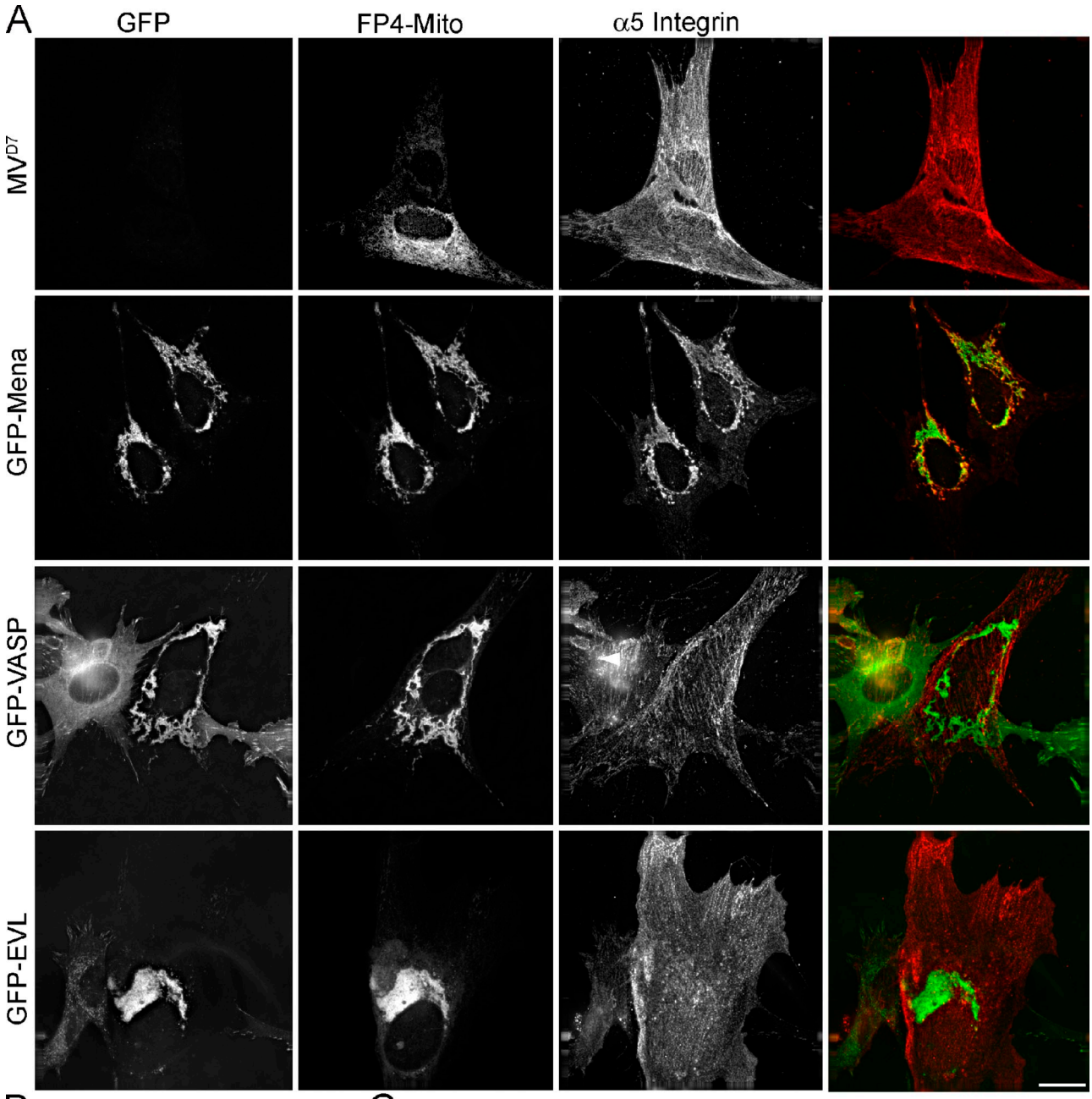

B

Pearson's correlation coefficient for colocaliation of mcherry-FP4-Mito and α5	
MV^{D7}	0.295 +/-0.076
MV^{D7} +Mena	0.987 +/-0.037 *
MV^{D7} +VASP	0.234 +/-0.098
MV^{D7} +EVL	0.259 +/-0.044

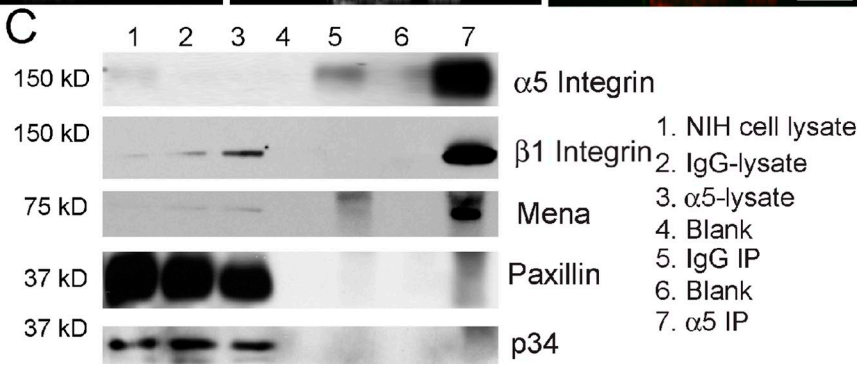

Figure 2. **Mena associates with α5, recruiting it to FP4-Mito–decorated mitochondria.** (A) MV^{D7} cells expressing mCherry-FP4-Mito alone (green), or GFP-tagged Mena, VASP, or EVL, and stained with anti-α5 (red). Bar, 10 μm. (B) Pearson's coefficients of colocalization of α5 with FP4-Mito. *, $P < 0.05$ from MV^{D7} cells. (C) Western blot analyses of anti-α5 immunoprecipitates from NIH3T3 cell lysates probed with anti-α5, -β1, -Mena, -Paxillin, and -p34 subunit of Arp2/3. "Lysate," 5% of total protein used for immunoprecipitation; "IgG," control antibody; blank lanes prevent carryover.

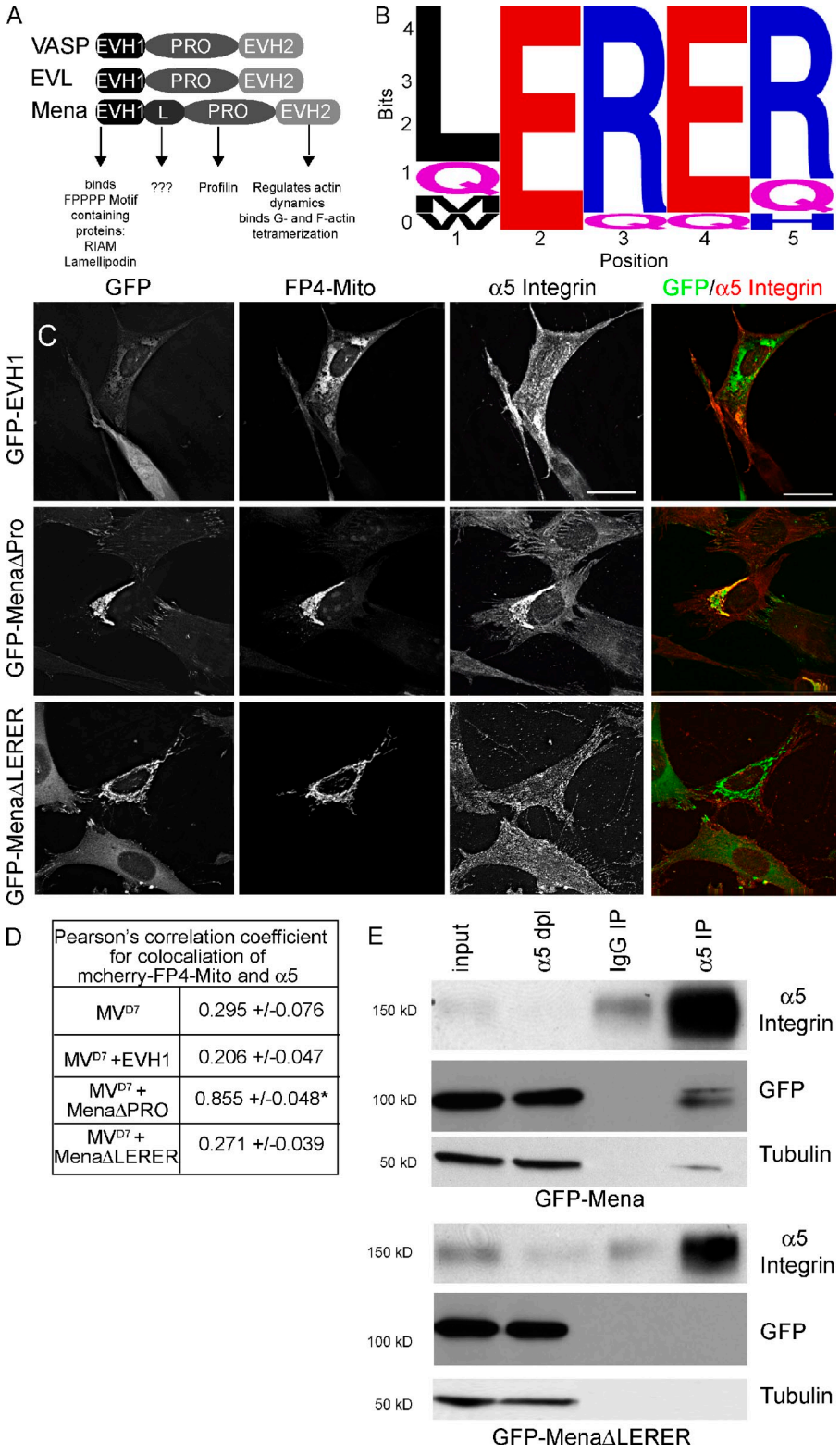

Figure 3. **LERER repeat region of Mena is required for interaction with α5.** (A) Ena/VASP domains. (B) Sequence motif schematic for LERER repeats in Mena; relative heights of each residue are proportional to their usage at given position. (C) α5 recruited to mitochondria in MV^{D7} cells that express indicated GFP-tagged Mena deletion mutants plus mCherry-FP4-Mito. (D) Pearson's coefficients of colocalization of α5 with FP4-Mito. *, $P < 0.05$ from MV^{D7}. (E) Anti-α5 immunoprecipitates from lysates of MV^{D7}+GFP-Mena (top) and MV^{D7}+GFP-MenaΔLERER (bottom) analyzed by Western blotting, probed with anti-α5, GFP, or tubulin. Input = 5% of lysate used for immunoprecipitation; "α5 dpl," 5% of supernatant sampled after α5 immunoprecipitation.

that contains GFP fused to its the α5 C terminus (α5-GFP; Laukaitis et al., 2001). In NIH3T3 cells cotransfected with α5-GFP and FP4-Mito, α5-GFP was not enriched significantly on the mitochondrial surface, whereas endogenous α5 was clearly recruited to FP4-Mito–decorated mitochondria (Fig. 4, D and E). To determine whether the GFP tag interfered with α5 recruitment in other fibroblast lines, FP4-Mito and α5-GFP were cotransfected into Rat2 fibroblasts and into primary mouse embryonic fibroblasts (MEFs): neither cell type showed significant recruitment of α5-GFP to mitochondria (Fig. S2 D). Although precise details of the interaction remain to be determined, these results indicate that the LERER repeat of Mena binds directly to α5 through an interaction that requires the C-terminal portion of α5.

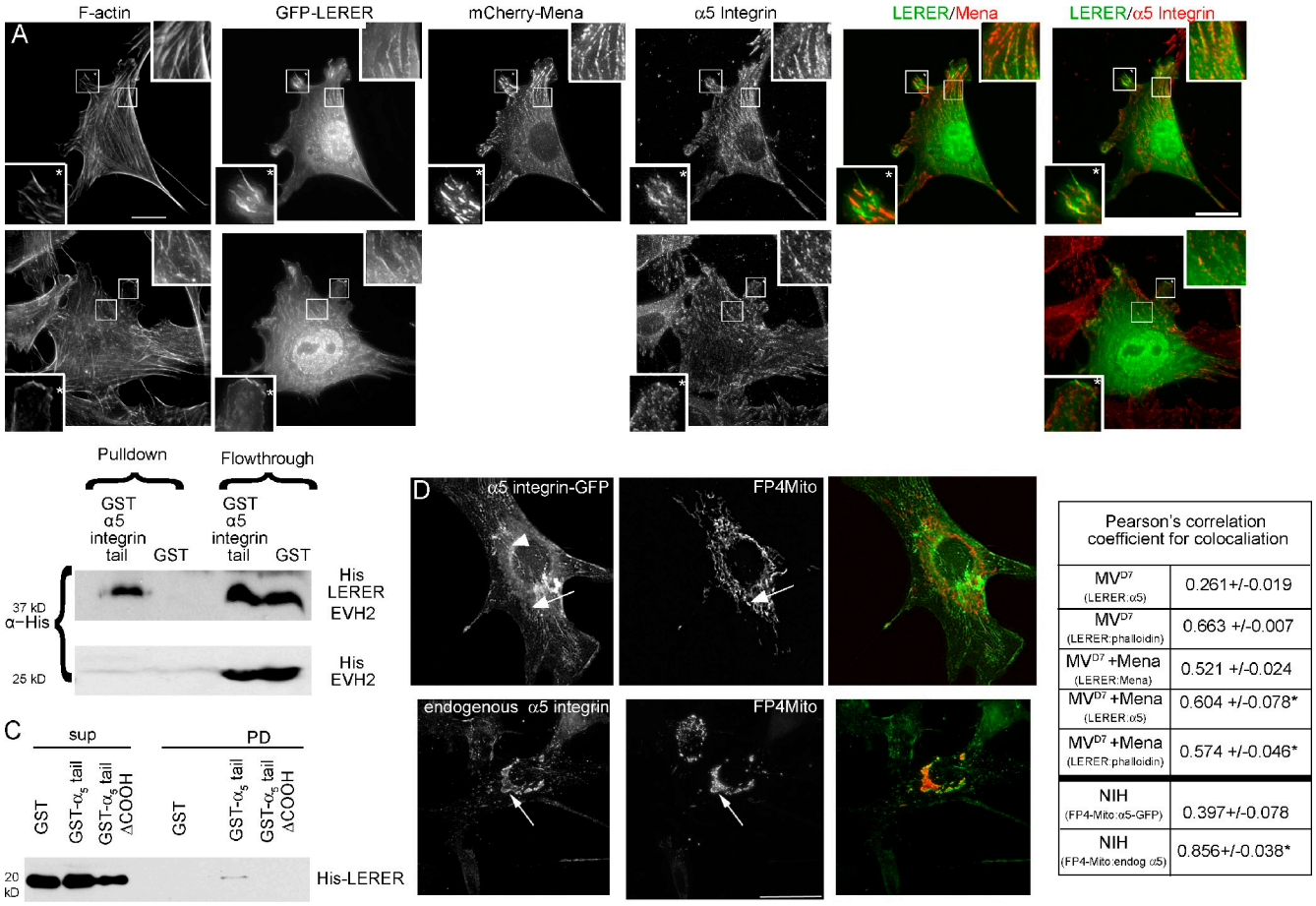

Pearson's correlation coefficient for colocaliation	
MV^{D7} (LERER:α5)	0.261+/-0.019
MV^{D7} (LERER:phalloidin)	0.663 +/-0.007
MV^{D7} +Mena (LERER:Mena)	0.521 +/-0.024
MV^{D7} +Mena (LERER:α5)	0.604 +/-0.078*
MV^{D7} +Mena (LERER:phalloidin)	0.574 +/-0.046*
NIH (FP4-Mito:α5-GFP)	0.397+/-0.078
NIH (FP4-Mito:endog α5)	0.856+/-0.038*

Figure 4. **LERER repeat region binds and localizes with α5.** (A) MV^{D7} cells expressing mCherry-Mena (top) and parental MV^{D7} cells expressing GFP-tagged LERER repeat (bottom). Top insets, region from cell center; bottom insets, regions from cell periphery. Insets show enlarged views of the boxed regions. (B) Western blot analysis of a GST binding assay with purified proteins. GST and GST-α5 cytoplasmic tail were incubated with His-tagged LERER-EVH2 or His-EVH2, and analyzed by a Western blot, probed with anti-His antibodies. (C) Binding assay with His-tagged LERER repeat and full-length α5 tail, or α5 tail lacking C-terminal amino acids (GST-α5 tailΔCOOH). (D) NIH3T3 cells expressing FP4-Mito and α5-GFP (top); Immunostaining for endogenous α5 (bottom) in an NIH3T3 cell expressing only FP4-Mito. Arrows, fiduciary markers for GFP-FP4-Mito; arrowheads, α5-GFP–positive adhesions (top). (E) Pearson's coefficients of colocalization of the indicated proteins from A and D. Bars, 10 μm.

Mena's LERER repeat modulates subcellular distribution of α5

Mena and α5β1 levels vary dynamically within cell–matrix adhesions as they mature during cell spreading and migration (Zaidel-Bar et al., 2003). We explored whether the Mena–α5 interaction influences the distribution of either molecule to the different types of adhesions. In fibroblasts cultured on FN, α5β1 is in nascent FXs, FAs, and FBs. In MV^{D7} cells that express GFP-Mena, Mena, α5, and paxillin colocalized extensively in peripheral FAs, whereas the cell center displayed robust α5 signal (typical of FBs), but little, if any, GFP-Mena (Fig. 5, A and C). When endogenous Mena was localized by immunofluorescence in fibroblasts transiently transfected with GFP-tensin (a major component of FBs; Zamir et al., 2000), we found only weak overlap of Mena with tensin in central FBs (Fig. 5 E).

Parental MV^{D7} cells contained peripheral FAs with α5 and paxillin, but lacked prominent FB-like α5 signal. Similarly, MV^{D7} cells expressing GFP-MenaΔLERER contained α5, paxillin, and GFP-MenaΔLERER within peripheral FAs, but lacked α5-positive FBs in the cell center (Fig. 5, A and C). The fraction of the ventral cell surface that contained α5 or paxillin was similar in MV^{D7} and GFP-MenaΔLERER cells, whereas in cells expressing GFP-Mena, the area of α5-positive adhesions was almost double relative to that of paxillin (Fig. 5 B). Surface levels of α5 were similar in adherent cells of both lines, as seen via FACS analyses with anti-α5 antibodies (Fig. 5 D) and via ELISA measurements of biotinylated α5 integrin (not shown), which indicates that altered distribution of α5 likely does not derive from defects in trafficking α5 to the cell surface, or maintaining it there. Thus, the LERER repeat is necessary for Mena-dependent formation or maintenance of α5-positive central FBs, normally a large fraction of the total area with α5-positive adhesions.

To confirm these results in another cell type, we isolated primary subdermal fibroblasts from perinatal VASP-null mice that were homozygous for a conditional Mena allele ($Mena^{Floxed}$), and examined the formation of α5-containing FBs after Mena deletion in culture. To excise the $Mena^{Floxed}$ allele, cells were infected with adenovirus that expressed either GFP-Cre recombinase or GFP alone (Fig. 6, A and C). In GFP-infected control fibroblasts, Mena and α5 colocalized at the leading edge and in

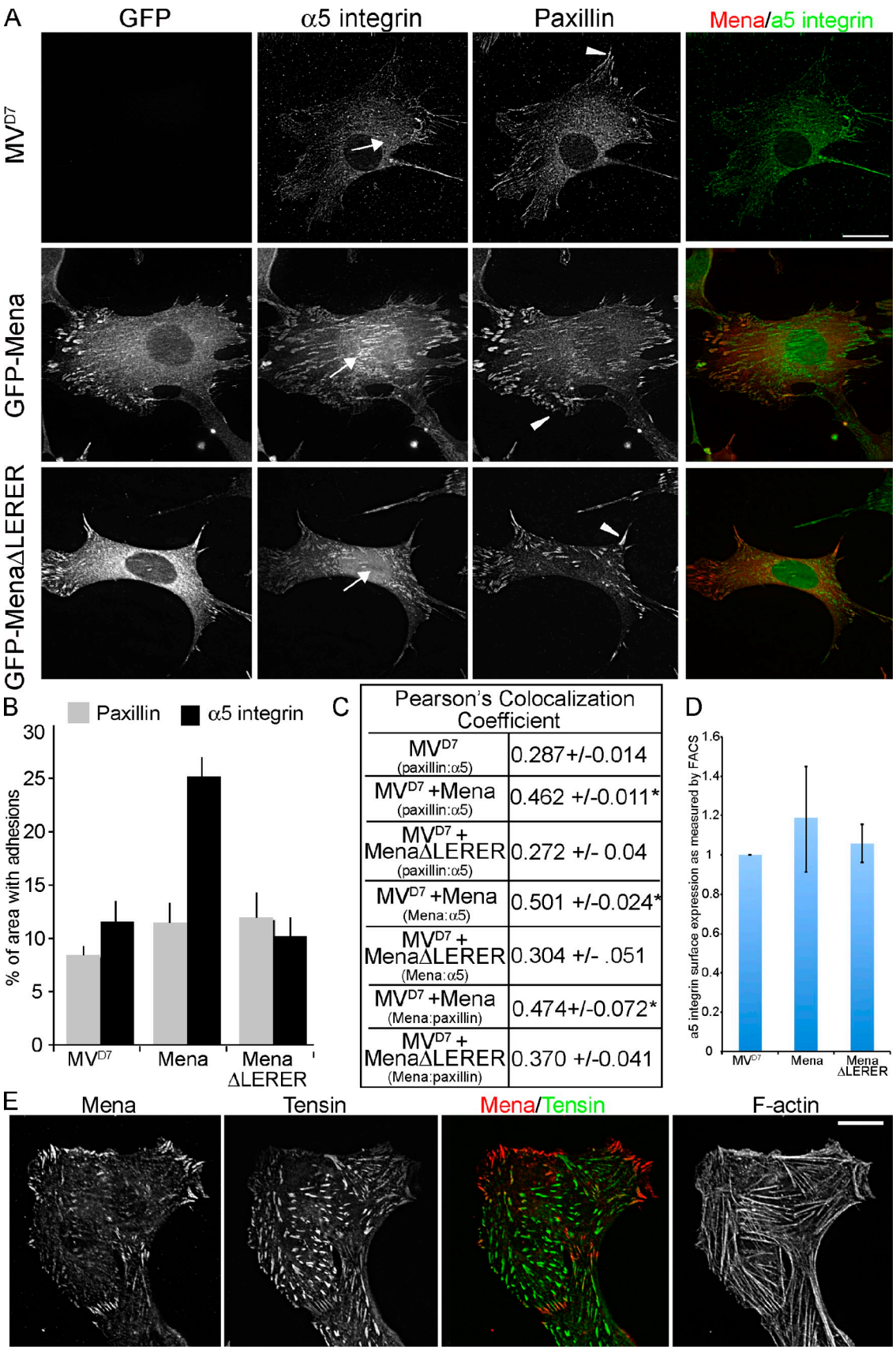

Figure 5. **Distribution of α5 to FBs requires Mena.** (A) MV^{D7} cells (top) and MV^{D7} cells expressing GFP-Mena (middle) or GFP-MenaΔLERER (bottom), plated on FN and stained for α5 and paxillin. Arrow, FBs in central region; arrowheads, FAs with peripheral paxillin. Bar, 10 µm. (B) Mean fraction of total cell area containing α5- or paxillin-positive ventral adhesions in MV^{D7} cells, and in MV^{D7} cells expressing GFP-Mena– or MenaΔLERER (**, $P < 0.01$).

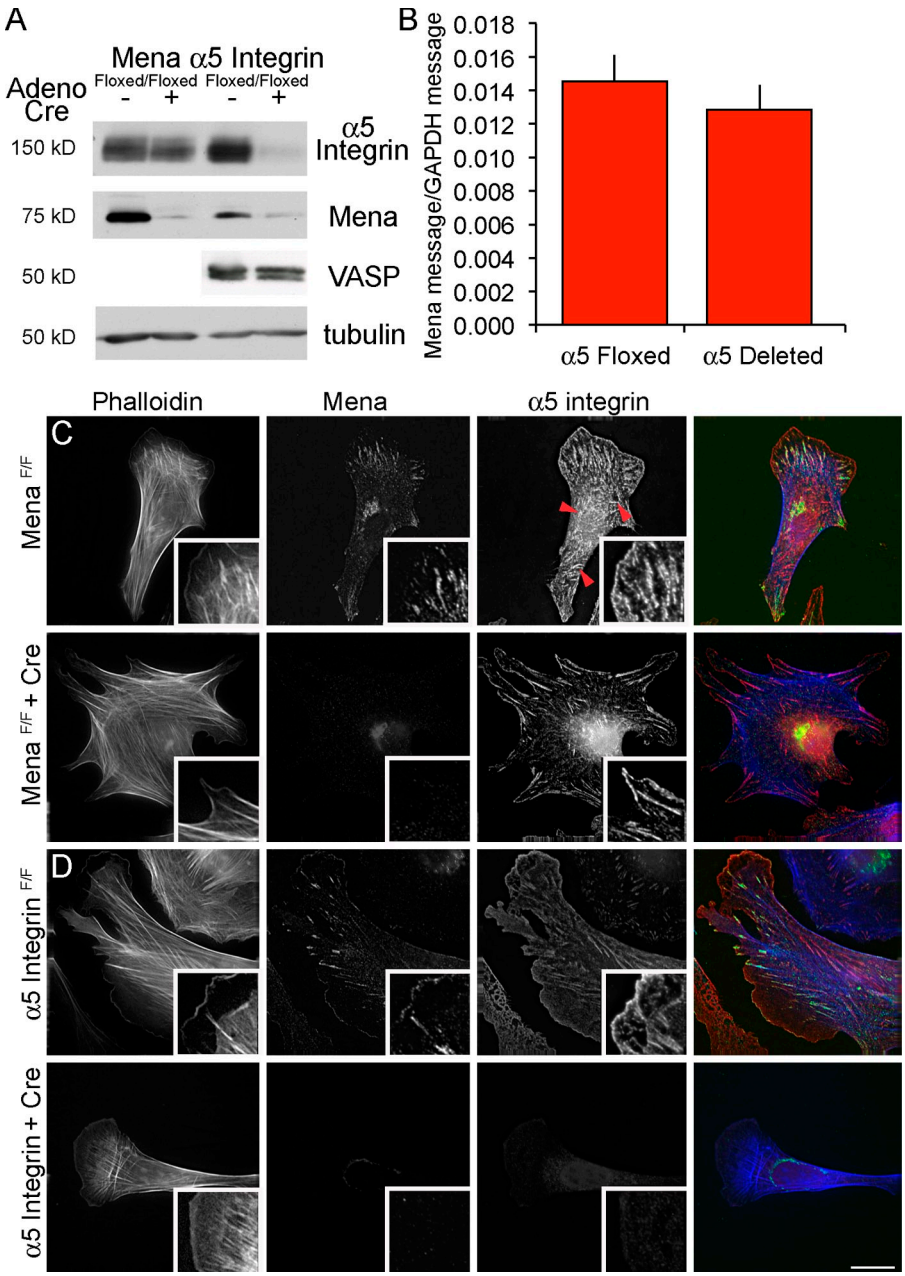

Figure 6. **Expression and distribution of Mena and α5 in cells lacking either protein.** (A) Western blots of lysates from subdermal fibroblasts isolated from Mena^{FLOXED} (Mena$^{F/F}$, homozygous for VASP deletion) or α5^{FLOXED} (α5$^{F/F}$) mice, 48 h after infection with GFP or GFP-Cre adenovirus, and probed with anti-α5, -Mena, -VASP, or -tubulin. (B) Quantitative PCR analysis of Mena mRNA levels in α5^{FLOXED} and α5-null fibroblasts. Immunofluorescence of Mena$^{F/F}$ (C) or α5$^{F/F}$ (D) cells after infection with GFP or GFP-Cre adenovirus. Panels on the right show enlarged views of the boxed regions. Error bars indicate mean ± SEM. Bar, 10 µm.

peripheral FAs; and α5, but not Mena, was also present in central FBs (Fig. 6 C). In Mena-deficient cells, α5 localized to the leading edge and in peripheral FAs, but not in central FB-like adhesions (Fig. 6 C). Therefore, central FB-like α5 adhesions are lost when Mena is absent in primary fibroblasts and MV^{D7} cells.

To test the effects of α5 deletion on Mena, primary subdermal fibroblasts isolated from perinatal mice homozygous for an α5^{Floxed} allele (van der Flier et al., 2010) were infected with Cre-expressing or control adenovirus (Fig. 6, A and D). Reduced α5 levels led to concomitant loss of Mena protein, but VASP levels were unaffected by the α5 deletion, indicating that the effect was specific to Mena and not to all Ena/VASP proteins. To determine whether loss of Mena results from reduced mRNA levels, we used quantitative reverse transcription PCR to analyze Cre-treated and control fibroblasts. We found that Mena mRNA levels were unaffected by α5 deletion (Fig. 6 B). Therefore, elimination of α5 in primary fibroblasts reduces Mena protein levels posttranscriptionally.

(C) Pearson's coefficients of colocalization of indicated proteins. *, P < 0.05 from MV^{D7} cells. (D) Surface α5 levels in MV^{D7} cells and MV^{D7} cells expressing GFP-Mena and GFP-MenaΔLERER. Cells were incubated with antibody to detect surface-exposed α5 by FACs analysis. Expression levels were normalized to fluorescence of GFP-expressing MV^{D7} cells, and averaged over three experiments. Error bars indicate mean ± SEM. P < 0.05. (E) Rat2 fibroblasts were transfected with GFP-tensin and stained for Mena. Bar, 15 µm.

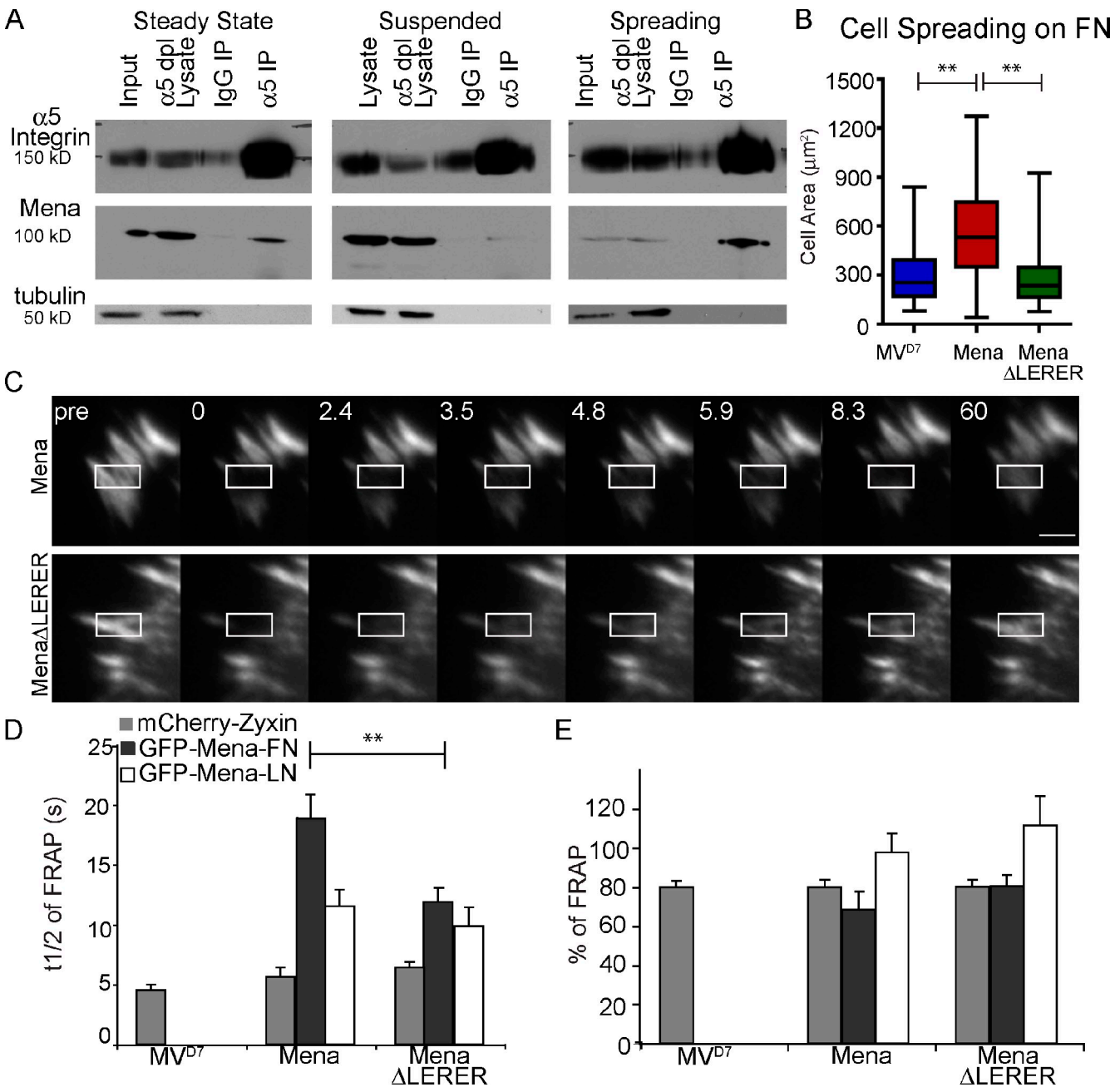

Figure 7. **Mena–α5 complex is enriched during cell spreading.** (A) Anti-α5 immunoprecipitates from lysates of MV^{D7}+GFP-Mena cells in steady-state culture, suspension, or 30 min after plating, were analyzed by Western blotting probed with the antibodies indicated. (B) Area of MV^{D7}, MV^{D7}+GFP-Mena, or MV^{D7}-GFP cells 30 min after plating on FN-coated coverslips. **, $P < 0.01$. (C) Examples of FRAP on MV^{D7} cells expressing GFP-Mena or GFP-MenaΔLERER 30 min after plating on FN. Fluorescence was photobleached (rectangles), and recovery was imaged over the indicated times. (D) The $t_{1/2}$ recovery of mCherry-zyxin or GFP-Mena of cells plated for 30 min on FN or laminin (LN). **, $P < 0.01$. (E) Percentage of total FRAP. Error bars indicate mean ± SEM.

Adhesion to FN increases the amount of Mena in complex with α5

The activation state of integrins often modulates their interactions with their cytosolic binding partners. To determine whether the Mena–α5 interaction is sensitive to α5β1 activation, we immunoprecipitated α5 from adherent, suspended, and spreading cells. 30 min after plating cells on FN, significantly more Mena was in complex with α5 (Fig. 7 A) compared with adherent cells in steady-state conditions. In contrast, the amount of Mena in complex with α5 was reduced in suspended cells.

We used established assays for α5β1 function in fibroblasts to test the hypothesis that adhesion-driven dynamics of the Mena–α5 complex have functional consequences. Fibroblast spreading on FN initiates the binding of integrins to FN, and rapid formation of actin polymerization–driven, adhesion-independent membrane extensions, followed by a distinct phase during which adhesions form dynamically and provide the traction required for further spreading (Zhang et al., 2008). We examined cell spreading on FN by measuring the area of MV^{D7}, MV^{D7}+GFP-Mena, or MV^{D7}+GFP-MenaΔLERER

cells 30 min after plating on FN-coated coverslips (Fig. 7 B and Fig. S3 A). MV^{D7} cells expressing GFP-Mena were significantly more spread ($P < 0.01$) compared with both MV^{D7} cells and MV^{D7}+GFP-MenaΔLERER cells, which spread equivalently. Therefore, adhesion-induced increases in the α5–Mena complex correlate with increased spreading on FN, supporting the possibility that direct interaction between α5 and Mena is required for optimal cell spreading.

Cell spreading requires actin polymerization, which is likely triggered by integrin-mediated signaling (Zhang et al., 2008). We tested whether Mena-dependent regulation of actin polymerization influences the effects of the α5–Mena complex on spreading by examining the spreading of MV^{D7} cells expressing a Mena mutant that lacks its F-actin binding site (MenaΔFAB, a motif required for Ena/VASP-dependent effects on actin polymerization). We observed that MenaΔFAB supports cell spreading to the same extent as Mena (Fig. S3 B). Spreading cells that express MenaΔFAB appeared to elaborate numerous filopodia-like protrusions, which is reminiscent of cells spreading in an anisotropic manner, whereas Mena-expressing cells appeared more like cells spreading in an isotropic mode (Fig. S3 A). Furthermore, the filopodia-like structures elaborated by GFP-MenaΔFAB cells exhibited GFP signal along the entire shaft rather than being concentrated at the distal tip of filopodia, as is typical of Mena (Dent et al., 2007). Although the mechanism underlying MenaΔFAB-dependent cell spreading remain to be determined, it is clear that Mena function in α5β1-dependent adhesion plays a more critical role in early cell spreading than does Mena-dependent actin polymerization.

As fibroblasts attach to and spread on FN, Mena localizes to the leading edge and to nascent β1-positive peripheral adhesions (Zhang et al., 2008). To determine if the adhesion-dependent increase in Mena interaction with α5 affects Mena stability in FAs during spreading, we used FRAP analysis to measure the recovery dynamics after photobleaching of GFP-Mena or GFP-MenaΔLERER in nascent, peripheral adhesions in cells plated for 30 min on FN (Fig. 7, C–E). The $t_{1/2}$ of FRAP was significantly greater for GFP-Mena than GFP-MenaΔLERER (18.9 ± 1.4 s vs. 11.9 ± 1.6 s, $P < 0.01$), but the overall percentage of FRAP was unchanged (Fig. 7 E). In contrast, the $t_{1/2}$ of FRAP of the FA component zyxin did not vary among the three cell types (Fig. 7 D). Zyxin binds Mena directly (Drees et al., 2000) and helps localize it to FAs (Hoffman et al., 2006), and we thus conclude that expression of the GFP-MenaΔLERER mutant does not induce a general perturbation of FA protein dynamics. Interestingly, the $t_{1/2}$ of FRAP of Mena and MenaΔLERER was equivalent 24 h after plating on FN (unpublished data). When plated for 30 min on laminin (LN), an ECM protein bound by a distinct set of integrins, the dynamics of both Mena and MenaΔLERER were equivalent to those observed for MenaΔLERER in cells plated for 30 min on FN. Collectively, these data indicate that FN binding by α5β1 during cell spreading reduces the turnover of Mena, and is dependent on its LERER repeat, which mediates direct binding to α5. Because tagging α5 with a fluorescent protein blocks interaction with Mena (Fig. 4), we were unable to ascertain how binding Mena affects the dynamics of α5 integrin.

Mena concentrates α5 and increases signaling within FAs

To determine whether Mena affects the amount of α5 within adhesions and signaling downstream of α5β1, we used immunofluorescence to measure the amount of α5, FAK phosphorylated at tyrosine 397 (pFAK397), paxillin phosphorylated at residue 118 (pPAX118), and global tyrosine phosphorylation (pY) specifically in Mena or MenaΔLERER containing peripheral adhesions in MV^{D7} cells (Fig. 8 A and Fig. S4). The signal intensity of α5 in GFP-Mena–positive FAs was significantly higher than in GFP-MenaΔLERER FAs (Fig. 8 B), which indicates that FAs containing Mena capable of binding α5 have higher concentrations of α5. Significantly higher levels of pFAK397 (Fig. 8 C), pPAX118 (Fig. 8 D), and pY (not depicted, $P < 0.001$) were observed in GFP-Mena–containing adhesions compared with GFP-MenaΔLERER FAs. No significant differences were observed (by either immunofluorescence or Western blotting) in levels of phosphor-FAK (pFAK), phosphor-paxillin (pPax), or pY throughout the whole cell between MV^{D7} cells expressing GFP-Mena versus GFP-MenaΔLERER (unpublished data); this indicates that differences in α5 and downstream signaling are spatially restricted to Mena-containing adhesions. Despite their ability to promote cell spreading, GFP-MenaΔFAB adhesions also contained lower levels of pFAK397 compared with GFP-Mena adhesions (Fig. S4), which suggests that the F-actin binding as well as α5 binding capabilities of Mena are required for normal FAK activation.

The Mena–α5 interaction is required for normal FN fibrillogenesis

During fibrillogenesis, α5β1 is attached to FN as it moves centripetally along stress fibers, forming FBs and generating the required tension (Pankov et al., 2000; Danen et al., 2002). Because central α5β1-positive FBs are absent in MV^{D7} and MenaΔLERER cells (Fig. 5), and pFAK is reduced (Fig. 8), we asked whether Mena–α5 and Mena–F-actin binding are required for α5β1-dependent FN fibrillogenesis. Parental MV^{D7} cells and MV^{D7} cells expressing GFP-Mena, GFP-MenaΔLERER, GFP-MenaΔFAB, or GFP-VASP (negative control) were plated overnight on vitronectin, then FN was added to the media for 4 h and cells were fixed and stained to identify FN fibrils (Fig. 9 and Fig. S5). MV^{D7}+GFP-Mena cells generated typical FN fibrils aligned with stress fibers and FBs, whereas parental MV^{D7} cells and MV^{D7} cells expressing either GFP-MenaΔLERER or GFP-VASP (Fig. 9 and Fig. S5) formed significantly less fibrillar FN, which suggests that the interaction between Mena and α5 is critical for efficient fibrillogenesis. Surprisingly, MenaΔFAB partially, but significantly, rescued fibrillogenesis (Fig. 9).

The Mena–α5 interaction influences cell motility

Because Mena and α5β1 exert context-dependent effects on cell motility, we explored how disrupting their interaction influences cell migration on FN. MV^{D7} cells exhibit a hypermotile phenotype, migrating twice as fast as MV^{D7} cells that express levels of GFP-Mena that are typical for fibroblasts (Bear et al., 2000).

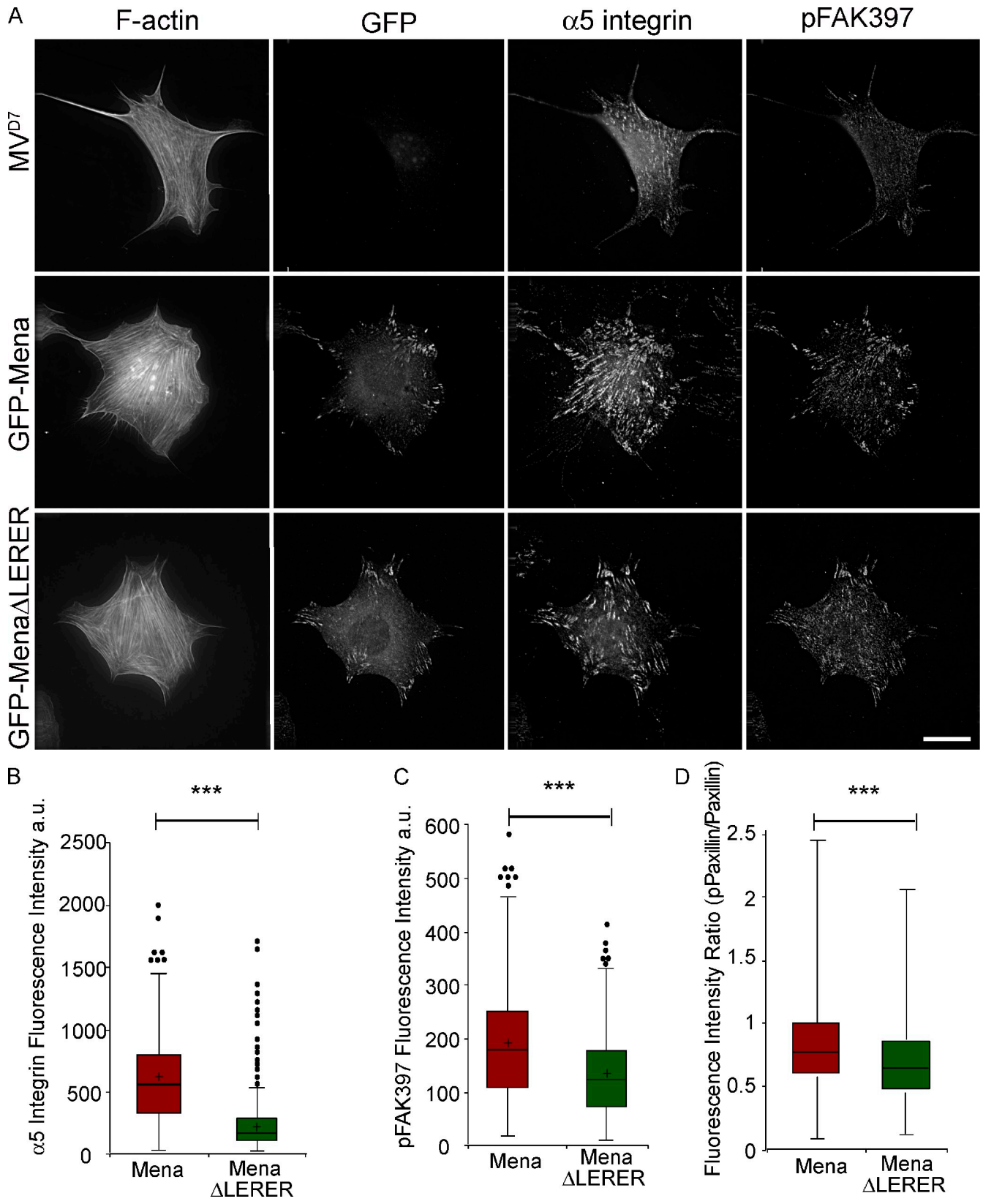

Figure 8. **Mena–α5 interaction modulates α5 density in adhesions and adhesion signaling.** (A) MV^{D7} cells and MV^{D7} cells expressing GFP-Mena or GFP-MenaΔLERER were plated on FN, then stained for α5 and FAK phosphorylated at Tyr397 (pFAK397). Bar, 10 µm. (B) Mean intensities of α5 immunofluorescence. (C and D) pFAK397 (C) and the ratio of pPaxillin/Paxillin (D) were measured in Mena and MenaΔLERER-containing adhesions: α5 intensity, pFAK levels, and the ratio of pPax118/Paxillin were significantly increased in Mena compared with MenaΔLERER-containing adhesions. ***, $P < 0.001$.

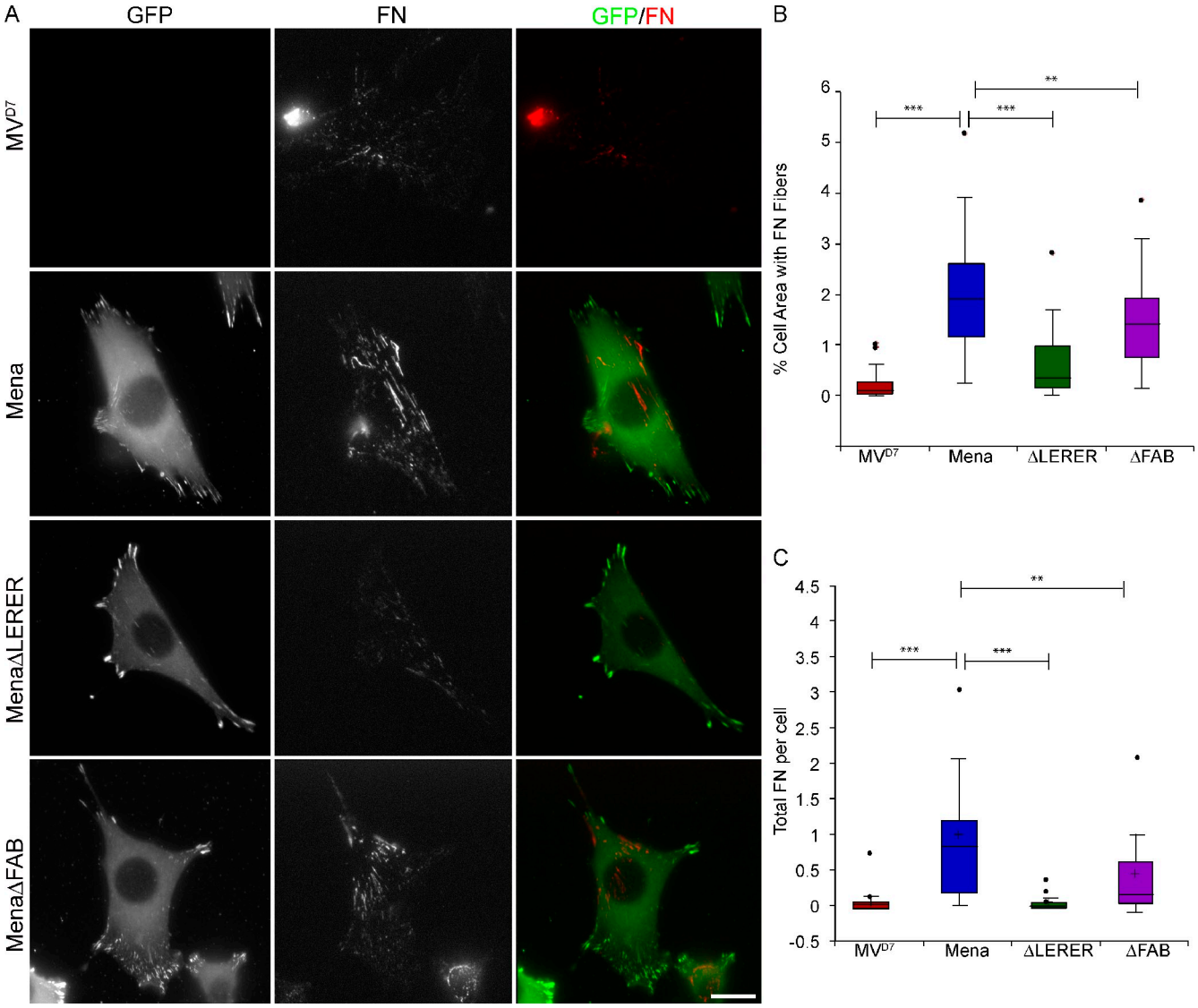

Figure 9. **Mena–α5 interaction, but not Mena–F-actin interaction, is necessary for normal fibrillogenesis.** (A) MV^{D7} cells and MV^{D7} cells expressing GFP-Mena, GFP-MenaΔLERER, or GFP-MenaΔFAB were plated on vitronectin overnight, and incubated with 10 µg/ml of fluorescently tagged FN for 4 h before fixation. Bar, 10 µm. (B) Percentage of cell area containing FN fibrils. (C) Total amount of FN within fibrils per cell. **, $P < 0.01$; ***, $P < 0.001$.

Time-lapse movies of parental and MV^{D7} cells expressing GFP-Mena and GFP-MenaΔLERER, and migrating on FN (Fig. 10), revealed that directional persistence of all three MV^{D7} cell lines is unaffected by expression of Mena or MenaΔLERER (not depicted), but that MV^{D7} cells migrate at the same rate as MV^{D7} cells expressing GFP-MenaΔLERER, which is about twice as fast as that of cells expressing GFP-Mena (Fig. 10 B). Thus, α5 binding is required for Mena-dependent MV^{D7} cell motility. To investigate motility in a more physiological context, we also tracked the movement of cells plated on cell-derived matrix (CDM; Cukierman et al., 2001), a 3D environment, and obtained results similar to those for the 2D migration assay on FN.

Discussion

Cell motility is a highly regulated, dynamic process that requires continual remodeling of the cytoskeleton as well as cell–cell and cell–matrix adhesions. Involvement of Ena/VASP in these processes has been demonstrated in a wide range of systems. Although Ena/VASP influences cellular protrusion dynamics by regulating actin polymerization through a mechanism of emerging focus (Bear and Gertler, 2009; Hansen and Mullins, 2010), how Ena/VASP affects adhesion is not well understood. Here we identify a direct connection between Mena and α5, and document that it is required for fibroblast spreading on FN, FB formation, and FN fibrillogenesis. We also show that the Mena–α5 interaction affects cell motility in 2D motility assays on planar FN, and in 3D assays in CDM, a FN-rich matrix produced by fibroblasts (Cukierman et al., 2001; Bass et al., 2007). Fibroblast motility in CDM is more dependent on α5β1 than on 2D FN surfaces. We conclude that the Mena–α5 interaction contributes to the physiological function of fibroblasts, which secrete and remodel ECM, and must migrate through interstitial ECM-rich 3D environments in vivo to perform essential functions.

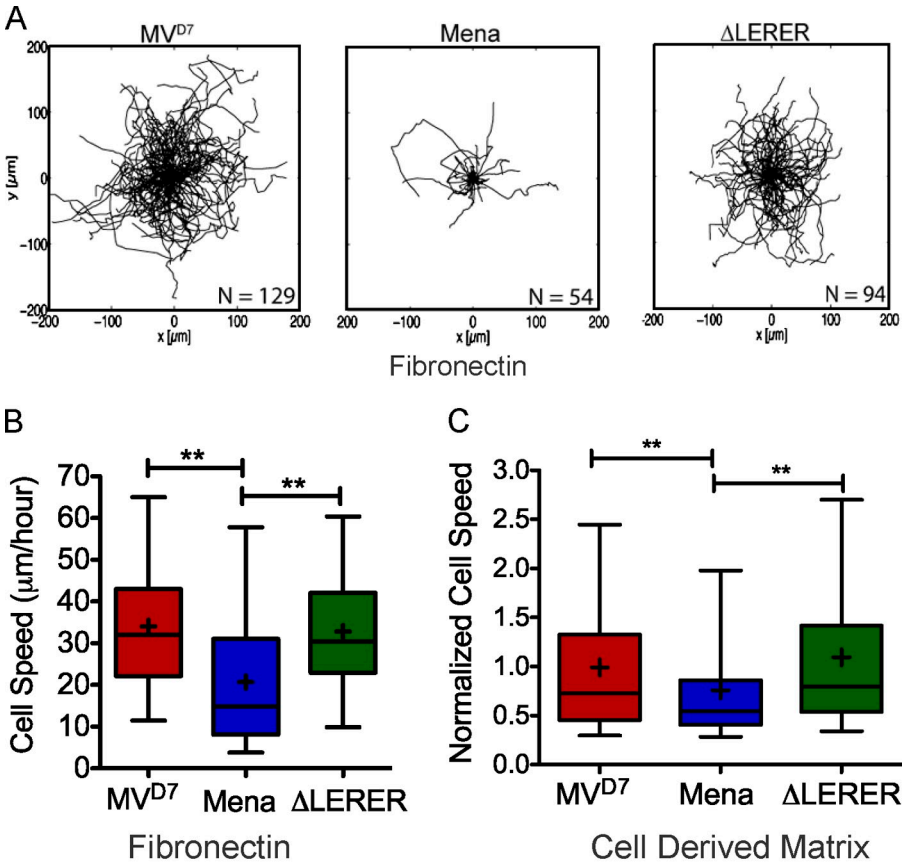

Figure 10. **Rescue of MV^{D7} hypermotility requires Mena capable of binding α5.** (A) Windrose plots of MV^{D7}, MV^{D7}+GFP-Mena, or GFP-MenaΔLERER cell tracks over a 6-h period. (B and C) Speed of indicated cells on FN for 6 h (B) and on CDM for 6 h (C). **, P < 0.01.

In addition to these roles in inside-out regulation of α5β1, the Mena–α5 complex is also regulated by, and necessary for, outside-in signaling by α5β1. Mena–α5 complex formation is driven by adhesion to FN. Mena binding to α5 also causes formation of FAs with higher concentrations of α5: this may reflect enhanced α5β1 clustering and binding to FN via increased avidity, though further work is needed to test this possibility. Mena binding to α5 is also necessary for signaling downstream of α5β1, as indicated by reductions in pFAK397, pPAX118, and global pY in adhesions that contain GFP-MenaΔLERER relative to those containing GFP-Mena. Based on these findings, we propose that Mena is a key modulator of α5β1-mediated bidirectional signaling between ECM and the actin cytoskeleton.

In primary fibroblasts that normally express both α5 and Mena, acute depletion of α5 causes a reduction in Mena levels either by blocking Mena translation or inducing its degradation. Consistent with this idea, integrins and FA proteins form complexes with the mRNA translation machinery (de Hoog et al., 2004; Humphries et al., 2009), and adhesion to FN triggers α5β1-dependent translation (Gorrini et al., 2005; Chung and Kim, 2008). FA proteins are also regulated by proteolytic enzymes (Franco and Huttenlocher, 2005) and by ubiquitin-mediated proteasome degradation (Huang et al., 2009). Mena and α5 are also normally expressed in cells that lack the other (e.g., cortical neurons contain Mena but lack α5; unpublished data), which suggests that cells expressing both proteins have specific regulatory mechanisms for coordinating levels of Mena with α5.

The Mena–α5 interaction requires the last 5 of the 28 residue α5 cytoplasmic tail, and is blocked by tagging the tail at its C terminus. Mena binds to α5 via the LERER repeat, a region spanning 91 or 121 amino acids with 13 or 15 repeats of the five-residue LERER motif in mouse and human, respectively. Whether each repeat binds an α5 tail is unknown, but multiple α5 tails could bind LERER repeats within each subunit of a Mena tetramer, raising the possibility that Mena clusters α5β1, thereby strengthening FN binding by increased avidity. Mena promotes actin polymerization in cell protrusions (Bear and Gertler, 2009), FAs, and sarcomeric units along F-actin bundles attached to FAs of endothelial cells (Furman et al., 2007). Given Mena's role in actin polymerization, it was surprising that MenaΔFAB, which does not bind F-actin or regulate actin dynamics, supports significant levels of FN fibrillogenesis; this suggests that Mena's role in this process can be, in part, uncoupled from its effects on actin dynamics. Mena may also link indirectly to the actin cytoskeleton by association with other FA components that bind F-actin. Direct Mena F-actin interaction is required to mediate α5β1 outside-in signaling that regulates pFAK397 levels.

Despite its role in fibrillogenesis, Mena is barely detectable in FBs compared with FAs, as are two other molecules important for fibrillogenesis: FAK (Ilić et al., 2004) and ILK (Zamir et al., 2000; Vouret-Craviari et al., 2004; Stanchi et al., 2009). Mena may cluster α5β1 and strengthen FN binding within FAs before α5β1–FN complexes begin moving toward central FBs. Alternatively, Mena–α5 interactions could target

FAs for maturation by changing α5 dynamics and stability within FAs. Consistent with the latter possibility, deletion of the LERER repeat increases turnover of Mena in nascent adhesions formed during cell spreading. A direct study of α5 dynamics and translocation was precluded by the inability of the α5-GFP construct (for live imaging of α5 dynamics; Laukaitis et al., 2001) to interact with Mena, likely because the construct blocked the LERER repeat from binding to the α5 cytoplasmic tail.

The inability of α5-GFP to bind Mena may perturb α5 function in some cell types and contexts. Clearly, α5-GFP, when expressed in α5-deficient CHO B2 cells, functions equivalently to untagged α5 in migration and spreading (Laukaitis et al., 2001). Some CHO cell lines (Benz et al., 2009), including CHO B2, lack detectable Mena protein (unpublished data); therefore, perturbation of Mena-dependent α5 function by GFP tagging would not be relevant in this cell type.

We find that use of the FP4-Mito system to block Ena/VASP function also blocks α5 function, which must be considered when using this tool in α5-expressing cells. Our laboratory and others have used FP4-Mito to study Ena/VASP function in a variety of systems; most conclusions from these studies have been validated by experiments conducted in MV^{D7} cells (Loureiro et al., 2002; Bear et al., 2002), primary neurons isolated from Mena/VASP/EVL triple-null embryos, or Ena mutant *Drosophila melanogaster* (lacking α5 and the LERER-repeat; Gates et al., 2007). However, FP4-Mito expression in flies causes a partial codepletion of Dia through association with Ena, possibly inducing phenotypic effects that may be more severe than the Ena null state (Homem and Peifer, 2009).

The LERER repeat is not found in VASP, EVL, or the invertebrate and *Dictyostelium discoideum* Ena/VASP orthologues. Interestingly, FN, α5β1, and the Mena LERER repeat are all vertebrate-specific adaptations (Whittaker et al., 2006), which suggests that they coevolved. The Mena–α5 interaction is highly regulated: loss of adhesion reduces the interaction whereas acute FN binding increases levels of the complex and the residence time of Mena within FAs. And though VASP does not bind any integrin subunit directly, it does promote inside-out activation of β1- and β2-containing integrins indirectly, via adaptor or signaling intermediates (Deevi et al., 2010). VASP functions in cross-regulation between αVβ3 and α5β1 (Worth et al., 2010): loss of β3 function reduces phosphorylation of a PKA-dependent site within VASP near its EVH1 domain, allowing it to bind FP4 repeats within RIAM, an adaptor that mediates Rap-GTPase-driven integrin activation (Lafuente et al., 2004). The VASP–RIAM complex associates with the β subunit–binding protein talin (Anthis and Campbell, 2011), causing α5β1 activation at peripheral adhesions (Worth et al., 2010); however, RIAM can also promote integrin activation by talin independently of Ena/VASP (Lafuente et al., 2004; Lee et al., 2009). The Mena EVH1 domain binds many of the same ligands as VASP (Ball et al., 2002), connecting Mena to integrins via RIAM or other FA proteins such as vinculin and zyxin that contain EVH1-binding sites and associate with β subunits indirectly. Juxtaposition of its EVH1 domain and LERER repeat may enable Mena to connect directly to α5 and indirectly to β1 simultaneously.

We show that rescue of the MV^{D7} hypermotile phenotype by GFP-Mena requires the LERER repeat; we have also reported that GFP-Mena and GFP-MenaΔLERER rescue the MV^{D7} hypermotility phenotype equivalently, as do GFP-VASP or GFP-EVL (Loureiro et al., 2002). We verify that GFP-MenaΔLERER is expressed stably, with a subcellular distribution similar to that of GFP-Mena (see also Loureiro et al., 2002). The divergent results may derive from differences in methods and reagents (including FN) used in the earlier study, or the use of cells adapted to CO_2-independent media as opposed to the current enclosed environmental chamber that we used for live-cell imaging. Our current sample size is also much larger: 372 MV^{D7} cells expressing GFP-MenaΔLERER from four separate 12-h time-lapse movies were analyzed, compared with 22 cells from two separate 4-h experiments in the older study.

Why is the LERER repeat required for Mena to rescue MV^{D7} cell spreading and motility? The interaction with α5β1 potentially allows Mena to influence cell motility through a variety of mechanisms, including modulation of adhesion strength and changes in outside-in signaling that affect other components of the motility machinery. Additionally, Ena/VASP deficiency reduces cellular capacity to generate actin-driven protrusive forces that drive lamellipodial and filopodial extension and propulsion of the intracellular pathogen *Listeria monocytogenes*, even though the actin networks formed during these processes are organized differently. Expression of Mena, VASP, or EVL rescues the actin polymerization–dependent phenotypes arising from deficiency of Ena/VASP in MV^{D7} cells or in primary neurons from triple Mena/VASP/EVL-null embryos (Loureiro et al., 2002; Geese et al., 2002; Applewhite et al., 2007; Dent et al., 2007). In general, Ena/VASP activity produces longer, sparsely branched filament networks; in the absence of stabilizing interconnections, these increasingly buckle against the membrane as they elongate because of their inherent flexibility (Mogilner and Oster, 2003). By coupling its stimulatory effect on barbed end elongation with its ability to bind and potentially cluster α5β1, Mena could present activated but unbound integrins right at the tips of lamellipodia and filopodia, which is consistent with the proposed "sticky fingers" mechanism for haptotaxis (Galbraith et al., 2007). In addition, through its role in FN remodeling, Mena may help form the interstitial fibrillar network that serves both as a migration substrate as well as a template that organizes growth factors and other ECM components into spatially organized cues. These cues elicit complex, coordinated responses (Hynes and Naba, 2012) when touched by the sticky fingers of cells in transit.

Recently, both α5β1 (Caswell et al., 2008; Valastyan et al., 2009; Muller et al., 2009) and Mena (Philippar et al., 2008; Robinson et al., 2009; Roussos et al., 2011a) have been implicated in breast cancer invasion and metastasis through effects on EGFR (Gertler and Condeelis, 2011). During tumor progression, changes in alternative splicing produce additional, functionally distinct Mena protein isoforms coexpressed with the canonical isoform. $Mena^{INV}$, a Mena isoform expressed in

a subpopulation of highly invasive, motile, and chemotactic tumor cells (Goswami et al., 2009), has been detected in breast cancer patients with invasive ductal carcinomas (Roussos et al., 2011b). Mena^{INV} expression promotes tumor cell invasion and metastasis by a mechanism involving increased tumor cell sensitivity to EGF (Philippar et. al. 2008; Roussos et al., 2011a). Interestingly, EGFR is sometimes found in complexes with α5β1 linked by their mutual cytosolic binding partner, RCP (Caswell et al., 2008; Muller et al., 2009). α5β1-RCP association with EGFR leads to coordinated recycling that targets α5β1 and EGFR to the front of cells, promotes 3D invasion, and dysregulates signaling downstream of both receptors. The potential functional and biochemical links between Mena^{INV} α5β1 and EGFR during tumor progression are an important topic for further investigation.

Materials and methods

Western blotting/immunoprecipitation

Standard procedures were used for protein electrophoresis, Western blotting, and immunoprecipitation. Western blots were developed with HRP-tagged secondary antibodies and ECL reagent (GE Healthcare). For α5 integrin immunoprecipitation, cells were lysed with intermittent agitation for 20 min at 4°C in CSK buffer (Humphries et al., 2009) and passed through a 23.5-gauge needle; the supernatant was saved after spinning for 15 min at 21,000 *g*. Lysates were precleared with protein A beads for 2 h, incubated with an α5 integrin antibody (1928; Millipore) for 2 h at 4°C, and then captured with BSA-blocked protein A beads for 2 h. Beads were washed three times in lysis buffer, and proteins were eluted in sample buffer. Western blots were probed with antibodies to: α5 integrin (sc-166681; Santa Cruz Biotechnology, Inc.), Mena (Lebrand et al., 2004), Paxillin (Signal Transduction laboratories), p34 (07-227; EMD Millipore), β1 integrin (1949; EMD Millipore), GFP (JL-8; Takara Bio Inc.), glyceraldehyde 3-phosphate dehydrogenase (GAPDH; 2118; Signal Transduction Laboratories), porin (A-21317; Molecular Probes), tubulin (DM1A), His tag (H1029; Sigma-Aldrich), pFAK397 (44625; Invitrogen), pTyr (4G10; EMD Millipore), and VASP polyclonal (Lanier et al., 1999). Function-blocking α5 antibody BIIG2 was purchased from the Developmental Studies Hybridoma bank and used at 20 µg/ml.

Mitochondrial purification

Mitochondria were isolated from NIH3T3 cells that expressed either FP4-Mito or DP4-Mito, with use of paramagnetic beads conjugated to an antibody specific for mitochondrial protein Tom34 (as per the manufacturer's instructions; Miltenyl Biotec).

Binding assays

GST-α5 constructs and His-tagged variants of the LERER repeat region were expressed and purified from *Escherichia coli*. 10 nM of α5 integrin cytoplasmic tail was immobilized on Glutathione beads and incubated at 4°C for 1 h, with 200 nM His-LERER variants at constant agitation in PBS with 0.1% Triton X-100 and 2 mM βME. Beads were washed three times, and proteins were eluted in sample buffer and assayed by Western blotting.

Microscopy

Cells were fixed for 20 min in 4% paraformaldehyde in PHEM buffer warmed to 37°C; they were permeabilized in 0.2% Triton X-100 and blocked in 10% donkey serum. Primary antibodies used for immunofluorescence include α5 integrin (1928; Millipore), integrin α4 [PS/2] (ab25247; Abcam), integrin αv [RMV-7] (ab63490; Abcam), integrin α6 [GoH3] (ab105669; Abcam), vinculin (Sigma-Aldrich), Mena, GFP (JL-8; Takara Bio Inc.), paxillin (610052; BD), Rab7 (9367S; Cell Signaling Technology), Rab11 (5589; Cell Signaling Technology), and EEA1 (3288S; Cell Signaling Technology). F-actin was stained with Alexa Fluor 647 and Alexa Fluor 350 Phalloidin (Invitrogen). Fluorochromes on secondary antibodies included Alexa Fluor 568, Alexa Fluor 488, Alexa Fluor 647, and Alexa Fluor 350 (Jackson ImmunoResearch Laboratories, Inc.). Cells were mounted in mounting media containing 90% glycerol and *n*-propyl-gallate, and imaged at room temperature. Z series of images were taken on a DeltaVision microscope (Applied Precision) using SoftWoRx acquisition software (Applied Precision), a 60× 1.3 NA Plan-Apochromat objective lens (Olympus), and a camera (CoolSNAP HQ; Photometrics). Images were deconvolved using Deltavision SoftWoRx software and objective specific point spread function.

FRAP of live cells was performed in culture media at 37°C, 5% CO_2 using a 405 laser in TIRF mode with a depth of 100 nm. Pre- and post-bleach Images were acquired with 488 and 561 solid-state laser on a microscope (Deltavision; Olympus) equipped with a 60× 1.3 NA Plan-Apochromat objective lens. A prebleach series of 10 images was collected at 10-s intervals, and the area of interest was bleached with 50% laser power. Acquisition settings were returned to prebleach settings, and images were taken with an adaptive time frame. Total elapsed time between the end of the prebleach series and the beginning of the postbleach series was 40–90 s (median 50 s).

Sequence analysis

The mouse Mena (ENAH) sequnce (Uniprot accession no. Q03173) was used to identify the repeat region as residues 175–252. These sequence regions were divided into chunks that fit one of several motifs: a five–amino acid motif roughly consistent with the form "L/M/Q-E-R/Q-E-R/Q," a seven–amino acid motif roughly consistent with the 5-mer motif with the last two amino acids of the motif repeated, and an eight–amino acid motif roughly consistent with the 5-mer motif preceded by a repetition of the first three amino acids of the motif. All sequences in the region of interest fell into one of these three motifs. A motif logo was generated for each species, making use of each instance of the 5-mer motif, the first five amino acids of the 7-mer motif, and the last five amino acids of the 8-mer motif using the program WebLogo.

Image analysis

Cell masks of cell area were made by thresholding phalloidin images. Subsequently, thresholding was done to evenly include adhesive structures between cells within these masks, and the intensity and area of these regions was measured. For analysis of photobleaching data, images were first corrected for overall photobleaching, and the integrated fluorescence intensity (Fr) inside a region that was smaller than the original bleached region by 4 pixels in x and y in each image was measured in the prebleach and recovery image series. Calculation of the $t_{1/2}$ for recovery and the percent fluorescence recovery was performed as described previously (Bulinski et al., 2001). In brief, cellular background was subtracted from these data, and the decay of fluorescence (photobleaching) over the same time period in an unbleached portion of a different adhesion was fitted with an exponential decay curve $[(F_{(t)} - F_0(e - kt)]$, in which $F_{(t)}$ is the fluorescence at any time, F_0 is the initial fluorescence, and k is the fluorescence decay constant. Decay-corrected FA fluorescence was plotted against time of recovery and fitted to an exponential recovery curve: $F = F_{inf} - [(F_{inf} - F_{blch})(e - kOFF(t))]$, in which F_{blch} is the fluorescence at the time of bleaching, and F_{inf} is the fluorescence at $t = \infty$ (that is, fluorescence completely recovered). This equation was used to determine k_{off}. The $t_{1/2}$ was calculated as $\ln(2)/k_{OFF}$ and the percent recovery was calculated as $[(F_{inf} - F_{blch})/(F_{prebleach} - F_{blch})] \times 100$.

Pearson's coefficients of colocalization were calculated using the Intensity Correlation Analysis Plugin available for ImageJ.

Statistical analysis

The paired Student's *t* test was used for statistical analyses of experiments with two conditions. In the cases of three or more conditions, analysis of variance (ANOVA) was used with the least significant difference post hoc test. Significant differences are indicated throughout as: *, $P < 0.05$; **, $P < 0.01$; and ***, $P < 0.001$.

Cell culture and plasmids

Coverslips were coated with 10 µg/ml bovine FN (Sigma-Aldrich) for 2 h at 37°C. Primary meningeal fibroblasts were cultured with cortical neurons, isolated from embryonic day 14.5 mice as described previously (Dent et al., 2007). In brief, cortices were microdissected, trypsinized for 30 min at 37°C, pelleted, and plated and maintained in neurobasal medium (Gibco) supplemented with B27 and L-Glutamine at 37°C, 5% CO_2. Perinatal subdermal fibroblasts were isolated from postnatal day 1 mice that harbored either floxed α5 integrin (van der Flier et al., 2010) or floxed Mena. Pups were washed in PBS, placed in 1% iodine for 1 min, following with 70% EtOH for 1 min, and washed twice in PBS. After decapitation, the skin was removed. Dermis and epidermis were separated by placing in

Eagle's minimal essential medium supplemented with 2.4 U/ml dispase (Roche) at 4°C overnight. Dermis was then separated and digested in 0.1% collagenase I + II in DME with 10% FBS for 30 min 37°C. They were then passed through a 70-mm filter, pelleted, and plated.

NIH3T3 cells, Rat2 cells, and perinatal fibroblasts were cultured in DME supplemented with 10% fetal bovine serum and maintained at 37°C, 5% CO_2. Parental MV^{D7} cells and MV^{D7} cells expressing tagged Mena and Mena mutants were maintained at 32°C, 5% CO_2 in DME supplemented with L-Glutamine, penicillin and streptomycin, 15% fetal bovine serum, and 50 U/ml interferon γ (I-4777; Sigma-Aldrich; Bear et al., 2000). mCherry-FP4-Mito, pMSCV-GFP-LERER, and peGFP-α5 integrin were introduced into MV^{D7}cells with use of Lonza nucleofection according to the manufacturer's instructions. pMSCV-GFP-LERER, pMSCV-GFP-MenaΔLERER, pGEX-GST-α5 cytoplasmic tail, pGEX-GST α5 cytoplasmic tail ΔCOOH, pQE80L-His-LERER, pQE80L-His-LERER-CoCo, pQE80L-His-LERER-EVH2, and pQE80L-His-EVH2 were cloned according to standard cloning procedures with N-terminal tags. N-terminally tagged mCherry-FP4-Mito has been described previously (Bear et al., 2000). N-terminally tagged GFP-tensin (full length, chicken) was a gift from K. Yamada (National Institutes of Health, Bethesda, MD) and was introduced into Rat2 cells with Lipofectamine 2000 (Invitrogen) according to the manufacturer's directions. GFP-α5 integrin (Laukaitis et al., 2001) was purchased from Addgene.

FN fibrillogenesis

FN-depleted medium was prepared as described previously (Pankov and Momchilova, 2009). In brief, 10 ml of gelatin Sepharose 4B was washed with sterile PBS three times. After removing the third wash, 10 ml of FBS was added, rocked for 30 min at room temperature, collected, aliquoted, and stored at −20°C. FN was fluorescently labeled with 549-NHS ester from Thermo Fisher Scientific (46407), as directed by the manufacturer. MV^{D7} cells were seeded on coverslips coated with 10 µg/ml vitronectin from Sigma-Aldrich (V9881) and allowed to adhere overnight. Medium was replaced with FN-depleted growth medium containing 10 µg/ml fluorescently labeled FN and incubated at 32°C for 4 h. Cells were then fixed and immunostained.

Motility analysis

MV^{D7} cells were stained with 1 µM CMFDA (Invitrogen) and seeded overnight in growth medium at 2,000 cells/cm^2 on FN (10 µg/ml)-coated coverglass. Media was replenished directly before imaging to facilitate addition of 10 µg/ml of α5 blocking antibody (5H10-27, MFR5; BD) where applicable. 2D migration was quantified by recording cell centroid displacement after live-cell imaging for 12 h (1 image/10 min) on an inverted microscope (Axiovert; Carl Zeiss) equipped with automatic stage positioning, a 5% CO_2, −37°C environmental chamber, fluorescent light source, and 10× Plan-Fluor objective lens. Resulting images were semiautomatically tracked using Imaris software (Bitplane, Inc.). A custom Matlab (Mathworks) script was used to calculate migration parameters and create wind-rose plots. Cell speed is reported for the final 6 h of the experiment to ensure steady state.

CDM

CDM were prepared as directed by King and Parsons (2011). In brief, primary human dermal fibroblasts (Lonza) were seeded at 50,000 cells/cm^2 on coverslips coated with cross-linked gelatin for 10 d in FGM2 media (Lonza) supplemented with 5 µg/ml FN and 35 µg/ml ascorbic acid. Cells were extracted with 20 mM NH4OH + 0.5% Triton X-100, and CDMs were washed extensively and kept at 4°C in PBS + penicillin/streptomycin. Matrix containing coverslips were placed in 12-well tissue culture plates and adhered with epoxy (3M). Fibroblasts (MV^{D7} variants; MV^{D7}, MV^{D7}-Mena, MV^{D7}-Mena-ΔLERER) were dyed with 1 µM CMFDA, then seeded on the CDM-containing coverslips at 2,500 cells/cm^2 and allowed to spread for 4–6 h before imaging. Coverslips were imaged every 15 min for 6 h at 37°C and 5% CO_2, at least eight images were captured per coverslip and four coverslips were imaged per condition.

α5 integrin surface levels

For assessment of α5 integrin surface levels, MV^{D7} fibroblasts were incubated on ice in 1% BSA, 2 mM EDTA in PBS with biotinylated α5 integrin antibody (557446; BD) or biotinylated rat IgG (012-060-003; Jackson ImmunoResearch Laboratories, Inc.) for 30 min. Cells were washed and incubated for 30 min on ice with APC streptavidin (554067; BD) and propidium iodide. Cells were washed, resuspended, and directly analyzed on a flow cytometer (FACSCalibur; BD). Biotinylation and analysis of surface levels of α5 integrin was performed as described previously (Caswell et al., 2008). In brief, cells were starved for 1 h, washed with PBS, and labeled with sulfo-NHS-SS-Biotin (Thermo Fisher Scientific) for 30 min at 4°C. Cells were lysed, and lysate was added overnight at 4°C to a BSA-blocked ELISA plate coated with α5 integrin antibodies. Lysate was removed and plates were extensively washed. Alexa Fluor 680–streptavidin was added to the plate 1 h at 4°C, washed, and developed using an Odyssey imaging system (Licor).

Generation of $Mena^{FLOXED}$ mice

A targeting vector was generated using pPGKneoF2L2DTA (Addgene). The construct contained a 1.1-kb short arm from intronic sequence 5′ to exon 2 of Mena with a loxp site at the end proximal to exon 2. Adjacent to this loxp site is a PGK-Neo resistance cassette flanked by FRT recombination sites. Next to this, a long arm consisting of a sequence containing Mena exon2 flanked by a loxp site followed by an addition 5 kb of intronic sequence 3′ to exon 2. A PGK-DTA cassette for negative selection was inserted outside of the short arm. The linearized targeting vector was electroporated into R1 embryonic stem (ES) cells. More than 1,000 G418-resistant ES colonies were picked and screened for homologous recombination by PCR. Five clones were identified, and homologous recombination was reconfirmed by Southern blotting. Standard methods were used to inject the targeted ES cells into blastocysts, generate chimeric animals, and finally identify germline transmission of the targeted allele (Kwiatkowski et al., 2007). The PGK-Neo cassette was excised by crossing to a transgenic "FLPer" that expresses FLP recombinase. The resulting allele, $Mena^{FLOXED}$, contains LoxP recombination sites flanking exon 2 of Mena. Introduction of CRE recombinase by transgene or in cultured primary cells causes excision of exon 2 generating a protein null allele.

Description of α5 FLOXED mice

A conditional α5 integrin targeting vector containing a thymidine kinase (TK) negative-selection cassette, an Frt-flanked PGK-neo cassette, and the 255-bp exon 1 of α5 integrin flanked by loxP sites was electroporated into R1 ES cells. These cells were selected and screened for correct recombination and single integration. The PGK-neo cassette was removed by transient expression of Flip recombinase. Two karyotyped, correctly targeted ES cell clones (2H2 and 3G3) gave germline transmission and identical results. Cre-mediated excision of exon 1 was confirmed by PCR genotyping and Southern blotting (van der Flier et al., 2010). Standard methods were used to inject the targeted ES cells into blastocysts, generate chimeric animals, and finally identify germline transmission of the targeted allele. The resulting allele, $\alpha5^{FLOXED}$, contains LoxP recombination sites flanking exon 1. Introduction of CRE recombinase by transgene or in cultured primary cells causes excision of exon 1, generating a protein-null allele.

Online supplemental material

Fig. S1 shows that FP4-Mito, but not DP4Mito, expression recruits Mena and α5. Fig. S2 is a supplement to Fig. 4 to show that the LERER repeat region binds α5, requires the C-terminal amino acids, and likely forms a coiled coil structure. Fig. S3 shows that α5, but not F-actin, binding is required for Mena to mediate efficient cell spreading. Fig. S4 shows that F-actin binding is required for high pFAK397 levels. Fig. S5 shows that FN fibrillogenesis in MV^{D7} cells is rescued by GFP-Mena but not GFP-VASP. Online supplemental material is available at http://www.jcb.org/cgi/content/full/jcb.201202079/DC1.

We thank Michele Balsamo and Arjan van der Flier for assistance with isolation of perinatal fibroblasts. GFP-Tensin was a gift from Ken Yamada to R.O. Hynes. We are grateful to Brian Joughin for generating the LERER sequence schematic, and Michele Balsamo, Aaron Meyer, Russell McConnell, Frauke Drees, Kwabena Badu-Nkansah, and John Lamar for helpful discussions.

This work was supported by National Institutes of Health grant GM58801 to F.B. Gertler, Howard Hughes Medical Institute funding to R.O. Hynes and National Cancer Institute grant U54-CA112967 to D.A. Lauffenburger, F.B. Gertler, and R.O. Hynes.

Submitted: 15 February 2012
Accepted: 17 July 2012

References

Anthis, N.J., and I.D. Campbell. 2011. The tail of integrin activation. *Trends Biochem. Sci.* 36:191–198. http://dx.doi.org/10.1016/j.tibs.2010.11.002

Applewhite, D.A., M. Barzik, S.-I. Kojima, T.M. Svitkina, F.B. Gertler, and G.G. Borisy. 2007. Ena/VASP proteins have an anti-capping independent

function in filopodia formation. *Mol. Biol. Cell*. 18:2579–2591. http://dx.doi.org/10.1091/mbc.E06-11-0990

Arjonen, A., J. Alanko, S. Veltel, and J. Ivaska. 2012. Distinct recycling of active and inactive β1 integrins. *Traffic*. In press.

Aszódi, A., A. Pfeifer, M. Ahmad, M. Glauner, X.H. Zhou, L. Ny, K.E. Andersson, B. Kehrel, S. Offermanns, and R. Fässler. 1999. The vasodilator-stimulated phosphoprotein (VASP) is involved in cGMP- and cAMP-mediated inhibition of agonist-induced platelet aggregation, but is dispensable for smooth muscle function. *EMBO J.* 18:37–48. http://dx.doi.org/10.1093/emboj/18.1.37

Ball, L.J., T. Jarchau, H. Oschkinat, and U. Walter. 2002. EVH1 domains: structure, function and interactions. *FEBS Lett.* 513:45–52. http://dx.doi.org/10.1016/S0014-5793(01)03291-4

Barzik, M., T.I. Kotova, H.N. Higgs, L. Hazelwood, D. Hanein, F.B. Gertler, and D.A. Schafer. 2005. Ena/VASP proteins enhance actin polymerization in the presence of barbed end capping proteins. *J. Biol. Chem.* 280:28653–28662. http://dx.doi.org/10.1074/jbc.M503957200

Bass, M.D., K.A. Roach, M.R. Morgan, Z. Mostafavi-Pour, T. Schoen, T. Muramatsu, U. Mayer, C. Ballestrem, J.P. Spatz, and M.J. Humphries. 2007. Syndecan-4-dependent Rac1 regulation determines directional migration in response to the extracellular matrix. *J. Cell Biol.* 177:527–538. http://dx.doi.org/10.1083/jcb.200610076

Bear, J.E., and F.B. Gertler. 2009. Ena/VASP: towards resolving a pointed controversy at the barbed end. *J. Cell Sci.* 122:1947–1953. http://dx.doi.org/10.1242/jcs.038125

Bear, J.E., J.J. Loureiro, I. Libova, R. Fässler, J. Wehland, and F.B. Gertler. 2000. Negative regulation of fibroblast motility by Ena/VASP proteins. *Cell*. 101:717–728. http://dx.doi.org/10.1016/S0092-8674(00)80884-3

Bear, J.E., T.M. Svitkina, M. Krause, D.A. Schafer, J.J. Loureiro, G.A. Strasser, I.V. Maly, O.Y. Chaga, J.A. Cooper, G.G. Borisy, and F.B. Gertler. 2002. Antagonism between Ena/VASP proteins and actin filament capping regulates fibroblast motility. *Cell*. 109:509–521. http://dx.doi.org/10.1016/S0092-8674(02)00731-6

Benz, P.M., C. Blume, S. Seifert, S. Wilhelm, J. Waschke, K. Schuh, F. Gertler, T. Münzel, and T. Renné. 2009. Differential VASP phosphorylation controls remodeling of the actin cytoskeleton. *J. Cell Sci.* 122:3954–3965. http://dx.doi.org/10.1242/jcs.044537

Boëda, B., D.C. Briggs, T. Higgins, B.K. Garvalov, A.J. Fadden, N.Q. McDonald, and M. Way. 2007. Tes, a specific Mena interacting partner, breaks the rules for EVH1 binding. *Mol. Cell*. 28:1071–1082. http://dx.doi.org/10.1016/j.molcel.2007.10.033

Bulinski, J.C., D.J. Odde, B.J. Howell, T.D. Salmon, and C.M. Waterman-Storer. 2001. Rapid dynamics of the microtubule binding of ensconsin in vivo. *J. Cell Sci.* 114:3885–3897.

Calderwood, D.A. 2004. Integrin activation. *J. Cell Sci.* 117:657–666. http://dx.doi.org/10.1242/jcs.01014

Caswell, P.T., M. Chan, A.J. Lindsay, M.W. McCaffrey, D. Boettiger, and J.C. Norman. 2008. Rab-coupling protein coordinates recycling of α5β1 integrin and EGFR1 to promote cell migration in 3D microenvironments. *J. Cell Biol.* 183:143–155. http://dx.doi.org/10.1083/jcb.200804140

Caswell, P.T., S. Vadrevu, and J.C. Norman. 2009. Integrins: masters and slaves of endocytic transport. *Nat. Rev. Mol. Cell Biol.* 10:843–853. http://dx.doi.org/10.1038/nrm2799

Chung, J., and T.H. Kim. 2008. Integrin-dependent translational control: Implication in cancer progression. *Microsc. Res. Tech.* 71:380–386. http://dx.doi.org/10.1002/jemt.20566

Clark, K., R. Pankov, M.A. Travis, J.A. Askari, A.P. Mould, S.E. Craig, P. Newham, K.M. Yamada, and M.J. Humphries. 2005. A specific alpha5beta1-integrin conformation promotes directional integrin translocation and fibronectin matrix formation. *J. Cell Sci.* 118:291–300. http://dx.doi.org/10.1242/jcs.01623

Cukierman, E., R. Pankov, D.R. Stevens, and K.M. Yamada. 2001. Taking cell-matrix adhesions to the third dimension. *Science*. 294:1708–1712. http://dx.doi.org/10.1126/science.1064829

Danen, E.H.J., P. Sonneveld, C. Brakebusch, R. Fässler, and A. Sonnenberg. 2002. The fibronectin-binding integrins alpha5beta1 and alphavbeta3 differentially modulate RhoA-GTP loading, organization of cell matrix adhesions, and fibronectin fibrillogenesis. *J. Cell Biol.* 159:1071–1086. http://dx.doi.org/10.1083/jcb.200205014

Deevi, R.K., M. Koney-Dash, A. Kissenpfennig, J.A. Johnston, K. Schuh, U. Walter, and K. Dib. 2010. Vasodilator-stimulated phosphoprotein regulates inside-out signaling of beta2 integrins in neutrophils. *J. Immunol.* 184:6575–6584. http://dx.doi.org/10.4049/jimmunol.0903910

de Hoog, C.L., L.J. Foster, and M. Mann. 2004. RNA and RNA binding proteins participate in early stages of cell spreading through spreading initiation centers. *Cell*. 117:649–662. http://dx.doi.org/10.1016/S0092-8674(04)00456-8

Dent, E.W., A.V. Kwiatkowski, L.M. Mebane, U. Philippar, M. Barzik, D.A. Rubinson, S. Gupton, J.E. Van Veen, C. Furman, J. Zhang, et al. 2007. Filopodia are required for cortical neurite initiation. *Nat. Cell Biol.* 9:1347–1359. http://dx.doi.org/10.1038/ncb1654

Dominguez, R. 2009. Actin filament nucleation and elongation factors—structure-function relationships. *Crit. Rev. Biochem. Mol. Biol.* 44:351–366. http://dx.doi.org/10.3109/10409230903277340

Drees, F., and F.B. Gertler. 2008. Ena/VASP: proteins at the tip of the nervous system. *Curr. Opin. Neurobiol.* 18:53–59. http://dx.doi.org/10.1016/j.conb.2008.05.007

Drees, B., E. Friederich, J. Fradelizi, D. Louvard, M.C. Beckerle, and R.M. Golsteyn. 2000. Characterization of the interaction between zyxin and members of the Ena/vasodilator-stimulated phosphoprotein family of proteins. *J. Biol. Chem.* 275:22503–22511. http://dx.doi.org/10.1074/jbc.M001698200

Ferron, F., G. Rebowski, S.H. Lee, and R. Dominguez. 2007. Structural basis for the recruitment of profilin-actin complexes during filament elongation by Ena/VASP. *EMBO J.* 26:4597–4606. http://dx.doi.org/10.1038/sj.emboj.7601874

Franco, S.J., and A. Huttenlocher. 2005. Regulating cell migration: calpains make the cut. *J. Cell Sci.* 118:3829–3838. http://dx.doi.org/10.1242/jcs.02562

Furman, C., A.L. Sieminski, A.V. Kwiatkowski, D.A. Rubinson, E. Vasile, R.T. Bronson, R. Fässler, and F.B. Gertler. 2007. Ena/VASP is required for endothelial barrier function in vivo. *J. Cell Biol.* 179:761–775. http://dx.doi.org/10.1083/jcb.200705002

Galbraith, C.G., K.M. Yamada, and J.A. Galbraith. 2007. Polymerizing actin fibers position integrins primed to probe for adhesion sites. *Science*. 315:992–995. http://dx.doi.org/10.1126/science.1137904

Gates, J., J.P. Mahaffey, S.L. Rogers, M. Emerson, E.M. Rogers, S.L. Sottile, D. Van Vactor, F.B. Gertler, and M. Peifer. 2007. Enabled plays key roles in embryonic epithelial morphogenesis in *Drosophila*. *Development*. 134:2027–2039. http://dx.doi.org/10.1242/dev.02849

Geese, M., J.J. Loureiro, J.E. Bear, J. Wehland, F.B. Gertler, and A.S. Sechi. 2002. Contribution of Ena/VASP proteins to intracellular motility of listeria requires phosphorylation and proline-rich core but not F-actin binding or multimerization. *Mol. Biol. Cell*. 13:2383–2396. http://dx.doi.org/10.1091/mbc.E02-01-0058

Geiger, B., and K.M. Yamada. 2011. Molecular architecture and function of matrix adhesions. *Cold Spring Harb. Perspect. Biol.* 3:a005033. http://dx.doi.org/10.1101/cshperspect.a005033

Gertler, F., and J. Condeelis. 2011. Metastasis: tumor cells becoming MENAcing. *Trends Cell Biol.* 21:81–90. http://dx.doi.org/10.1016/j.tcb.2010.10.001

Gertler, F.B., K. Niebuhr, M. Reinhard, J. Wehland, and P. Soriano. 1996. Mena, a relative of VASP and *Drosophila* Enabled, is implicated in the control of microfilament dynamics. *Cell*. 87:227–239. http://dx.doi.org/10.1016/S0092-8674(00)81341-0

Gorrini, C., F. Loreni, V. Gandin, L.A. Sala, N. Sonenberg, P.C. Marchisio, and S. Biffo. 2005. Fibronectin controls cap-dependent translation through beta1 integrin and eukaryotic initiation factors 4 and 2 coordinated pathways. *Proc. Natl. Acad. Sci. USA*. 102:9200–9205. http://dx.doi.org/10.1073/pnas.0409513102

Goswami, S., U. Philippar, D. Sun, A. Patsialou, J. Avraham, W. Wang, F. Di Modugno, P. Nistico, F.B. Gertler, and J.S. Condeelis. 2009. Identification of invasion specific splice variants of the cytoskeletal protein Mena present in mammary tumor cells during invasion in vivo. *Clin. Exp. Metastasis*. 26:153–159. http://dx.doi.org/10.1007/s10585-008-9225-8

Gupton, S.L., and F.B. Gertler. 2010. Integrin signaling switches the cytoskeletal and exocytic machinery that drives neuritogenesis. *Dev. Cell*. 18:725–736. http://dx.doi.org/10.1016/j.devcel.2010.02.017

Hansen, S.D., and R.D. Mullins. 2010. VASP is a processive actin polymerase that requires monomeric actin for barbed end association. *J. Cell Biol.* 191:571–584. http://dx.doi.org/10.1083/jcb.201003014

Hauser, W., K.P. Knobeloch, M. Eigenthaler, S. Gambaryan, V. Krenn, J. Geiger, M. Glazova, E. Rohde, I. Horak, U. Walter, and M. Zimmer. 1999. Megakaryocyte hyperplasia and enhanced agonist-induced platelet activation in vasodilator-stimulated phosphoprotein knockout mice. *Proc. Natl. Acad. Sci. USA*. 96:8120–8125. http://dx.doi.org/10.1073/pnas.96.14.8120

Hoffman, L.M., C.C. Jensen, S. Kloeker, C.-L.A. Wang, M. Yoshigi, and M.C. Beckerle. 2006. Genetic ablation of zyxin causes Mena/VASP mislocalization, increased motility, and deficits in actin remodeling. *J. Cell Biol.* 172:771–782. http://dx.doi.org/10.1083/jcb.200512115

Homem, C.C.F., and M. Peifer. 2009. Exploring the roles of diaphanous and enabled activity in shaping the balance between filopodia and lamellipodia. *Mol. Biol. Cell*. 20:5138–5155. http://dx.doi.org/10.1091/mbc.E09-02-0144

Huang, C., Z. Rajfur, N. Yousefi, Z. Chen, K. Jacobson, and M.H. Ginsberg. 2009. Talin phosphorylation by Cdk5 regulates Smurf1-mediated talin head ubiquitylation and cell migration. *Nat. Cell Biol.* 11:624–630. http://dx.doi.org/10.1038/ncb1868

Humphries, J.D., A. Byron, M.D. Bass, S.E. Craig, J.W. Pinney, D. Knight, and M.J. Humphries. 2009. Proteomic analysis of integrin-associated complexes identifies RCC2 as a dual regulator of Rac1 and Arf6. *Sci. Signal.* 2:ra51. http://dx.doi.org/10.1126/scisignal.2000396

Huttenlocher, A., and A.R. Horwitz. 2011. Integrins in cell migration. *Cold Spring Harb. Perspect. Biol.* 3:a005074. http://dx.doi.org/10.1101/cshperspect.a005074

Hynes, R.O. 2002. Integrins: bidirectional, allosteric signaling machines. *Cell*. 110:673–687. http://dx.doi.org/10.1016/S0092-8674(02)00971-6

Hynes, R.O. 2009. The extracellular matrix: not just pretty fibrils. *Science*. 326:1216–1219. http://dx.doi.org/10.1126/science.1176009

Hynes, R.O., and A. Naba. 2012. Overview of the matrisome—an inventory of extracellular matrix constituents and functions. *Cold Spring Harb. Perspect. Biol.* 4:a004903. http://dx.doi.org/10.1101/cshperspect.a004903

Ilić, D., B. Kovacic, K. Johkura, D.D. Schlaepfer, N. Tomasević, Q. Han, J.-B. Kim, K. Howerton, C. Baumbusch, N. Ogiwara, et al. 2004. FAK promotes organization of fibronectin matrix and fibrillar adhesions. *J. Cell Sci.* 117:177–187. http://dx.doi.org/10.1242/jcs.00845

Ivaska, J., and J. Heino. 2011. Cooperation between integrins and growth factor receptors in signaling and endocytosis. *Annu. Rev. Cell Dev. Biol.* 27:291–320. http://dx.doi.org/10.1146/annurev-cellbio-092910-154017

King, S.J., and M. Parsons. 2011. Imaging cells within 3D cell-derived matrix. *Methods Mol. Biol.* 769:53–64. http://dx.doi.org/10.1007/978-1-61779-207-6_5

Kwiatkowski, A.V., D.A. Rubinson, E.W. Dent, J. Edward van Veen, J.D. Leslie, J. Zhang, L.M. Mebane, U. Philippar, E.M. Pinheiro, A.A. Burds, et al. 2007. Ena/VASP Is Required for neuritogenesis in the developing cortex. *Neuron*. 56:441–455. http://dx.doi.org/10.1016/j.neuron.2007.09.008

Lafuente, E.M., A.A. van Puijenbroek, M. Krause, C.V. Carman, G.J. Freeman, A. Berezovskaya, E. Constantine, T.A. Springer, F.B. Gertler, and V.A. Boussiotis. 2004. RIAM, an Ena/VASP and Profilin ligand, interacts with Rap1-GTP and mediates Rap1-induced adhesion. *Dev. Cell*. 7:585–595. http://dx.doi.org/10.1016/j.devcel.2004.07.021

Lanier, L.M., M.A. Gates, W. Witke, A.S. Menzies, A.M. Wehman, J.D. Macklis, D. Kwiatkowski, P. Soriano, and F.B. Gertler. 1999. Mena is required for neurulation and commissure formation. *Neuron*. 22:313–325. http://dx.doi.org/10.1016/S0896-6273(00)81092-2

Laukaitis, C.M., D.J. Webb, K. Donais, and A.F. Horwitz. 2001. Differential dynamics of alpha 5 integrin, paxillin, and alpha-actinin during formation and disassembly of adhesions in migrating cells. *J. Cell Biol.* 153:1427–1440. http://dx.doi.org/10.1083/jcb.153.7.1427

Lebrand, C., E.W. Dent, G.A. Strasser, L.M. Lanier, M. Krause, T.M. Svitkina, G.G. Borisy, and F.B. Gertler. 2004. Critical role of Ena/VASP proteins for filopodia formation in neurons and in function downstream of netrin-1. *Neuron*. 42:37–49. http://dx.doi.org/10.1016/S0896-6273(04)00108-4

Lee, H.-S., C.J. Lim, W. Puzon-McLaughlin, S.J. Shattil, and M.H. Ginsberg. 2009. RIAM activates integrins by linking talin to ras GTPase membrane-targeting sequences. *J. Biol. Chem.* 284:5119–5127. http://dx.doi.org/10.1074/jbc.M807117200

Loureiro, J.J., D.A. Rubinson, J.E. Bear, G.A. Baltus, A.V. Kwiatkowski, and F.B. Gertler. 2002. Critical roles of phosphorylation and actin binding motifs, but not the central proline-rich region, for Ena/vasodilator-stimulated phosphoprotein (VASP) function during cell migration. *Mol. Biol. Cell*. 13:2533–2546. http://dx.doi.org/10.1091/mbc.E01-10-0102

Margadant, C., H.N. Monsuur, J.C. Norman, and A. Sonnenberg. 2011. Mechanisms of integrin activation and trafficking. *Curr. Opin. Cell Biol.* 23:607–614. http://dx.doi.org/10.1016/j.ceb.2011.08.005

McAnulty, R.J. 2007. Fibroblasts and myofibroblasts: their source, function and role in disease. *Int. J. Biochem. Cell Biol.* 39:666–671. http://dx.doi.org/10.1016/j.biocel.2006.11.005

Mogilner, A., and G. Oster. 2003. Polymer motors: pushing out the front and pulling up the back. *Curr. Biol.* 13:R721–R733. http://dx.doi.org/10.1016/j.cub.2003.08.050

Moser, M., K.R. Legate, R. Zent, and R. Fässler. 2009. The tail of integrins, talin, and kindlins. *Science*. 324:895–899. http://dx.doi.org/10.1126/science.1163865

Muller, P.A.J., P.T. Caswell, B. Doyle, M.P. Iwanicki, E.H. Tan, S. Karim, N. Lukashchuk, D.A. Gillespie, R.L. Ludwig, P. Gosselin, et al. 2009. Mutant p53 drives invasion by promoting integrin recycling. *Cell*. 139:1327–1341. http://dx.doi.org/10.1016/j.cell.2009.11.026

Pankov, R., and A. Momchilova. 2009. Fluorescent labeling techniques for investigation of fibronectin fibrillogenesis (labeling fibronectin fibrillogenesis). *Methods Mol. Biol.* 522:261–274. http://dx.doi.org/10.1007/978-1-59745-413-1_18

Pankov, R., E. Cukierman, B.Z. Katz, K. Matsumoto, D.C. Lin, S. Lin, C. Hahn, and K.M. Yamada. 2000. Integrin dynamics and matrix assembly: tensin-dependent translocation of α(5)β(1) integrins promotes early fibronectin fibrillogenesis. *J. Cell Biol.* 148:1075–1090. http://dx.doi.org/10.1083/jcb.148.5.1075

Philippar, U., E.T. Roussos, M. Oser, H. Yamaguchi, H.-D. Kim, S. Giampieri, Y. Wang, S. Goswami, J.B. Wyckoff, D.A. Lauffenburger, et al. 2008. A Mena invasion isoform potentiates EGF-induced carcinoma cell invasion and metastasis. *Dev. Cell*. 15:813–828. http://dx.doi.org/10.1016/j.devcel.2008.09.003

Pula, G., and M. Krause. 2008. Role of Ena/VASP proteins in homeostasis and disease. *Handb Exp Pharmacol*. 186:39–65. http://dx.doi.org/10.1007/978-3-540-72843-6_3

Rantala, J.K., J. Pouwels, T. Pellinen, S. Veltel, P. Laasola, E. Mattila, C.S. Potter, T. Duffy, J.P. Sundberg, O. Kallioniemi, et al. 2011. SHARPIN is an endogenous inhibitor of β1-integrin activation. *Nat. Cell Biol.* 13:1315–1324. http://dx.doi.org/10.1038/ncb2340

Robinson, B.D., G.L. Sica, Y.-F. Liu, T.E. Rohan, F.B. Gertler, J.S. Condeelis, and J.G. Jones. 2009. Tumor microenvironment of metastasis in human breast carcinoma: a potential prognostic marker linked to hematogenous dissemination. *Clin. Cancer Res.* 15:2433–2441. http://dx.doi.org/10.1158/1078-0432.CCR-08-2179

Roussos, E.T., M. Balsamo, S.K. Alford, J.B. Wyckoff, B. Gligorijevic, Y. Wang, M. Pozzuto, R. Stobezki, S. Goswami, J.E. Segall, et al. 2011a. Mena invasive (MenaINV) promotes multicellular streaming motility and transendothelial migration in a mouse model of breast cancer. *J. Cell Sci.* 124:2120–2131. http://dx.doi.org/10.1242/jcs.086231

Roussos, E.T., S. Goswami, M. Balsamo, Y. Wang, R. Stobezki, E. Adler, B.D. Robinson, J.G. Jones, F.B. Gertler, J.S. Condeelis, and M.H. Oktay. 2011b. Mena invasive (Mena(INV)) and Mena11a isoforms play distinct roles in breast cancer cell cohesion and association with TMEM. *Clin. Exp. Metastasis*. 28:515–527. http://dx.doi.org/10.1007/s10585-011-9388-6

Schwarzbauer, J.E., and D.W. DeSimone. 2011. Fibronectins, their fibrillogenesis, and in vivo functions. *Cold Spring Harb. Perspect. Biol.* 3:a005041. http://dx.doi.org/10.1101/cshperspect.a005041

Singh, P., C. Carraher, and J.E. Schwarzbauer. 2010. Assembly of fibronectin extracellular matrix. *Annu. Rev. Cell Dev. Biol.* 26:397–419. http://dx.doi.org/10.1146/annurev-cellbio-100109-104020

Stanchi, F., C. Grashoff, C.F. Nguemeni Yonga, D. Grall, R. Fässler, and E. Van Obberghen-Schilling. 2009. Molecular dissection of the ILK-PINCH-parvin triad reveals a fundamental role for the ILK kinase domain in the late stages of focal-adhesion maturation. *J. Cell Sci.* 122:1800–1811. http://dx.doi.org/10.1242/jcs.044602

Valastyan, S., N. Benaich, A. Chang, F. Reinhardt, and R.A. Weinberg. 2009. Concomitant suppression of three target genes can explain the impact of a microRNA on metastasis. *Genes Dev.* 23:2592–2597. http://dx.doi.org/10.1101/gad.1832709

van der Flier, A., K. Badu-Nkansah, C.A. Whittaker, D. Crowley, R.T. Bronson, A. Lacy-Hulbert, and R.O. Hynes. 2010. Endothelial alpha5 and alphav integrins cooperate in remodeling of the vasculature during development. *Development*. 137:2439–2449. http://dx.doi.org/10.1242/dev.049551

Vicente-Manzanares, M., and A.R. Horwitz. 2011. Adhesion dynamics at a glance. *J. Cell Sci.* 124:3923–3927. http://dx.doi.org/10.1242/jcs.095653

Vouret-Craviari, V., E. Boulter, D. Grall, C. Matthews, and E. Van Obberghen-Schilling. 2004. ILK is required for the assembly of matrix-forming adhesions and capillary morphogenesis in endothelial cells. *J. Cell Sci.* 117:4559–4569. http://dx.doi.org/10.1242/jcs.01331

Whittaker, C.A., K.-F. Bergeron, J. Whittle, B.P. Brandhorst, R.D. Burke, and R.O. Hynes. 2006. The echinoderm adhesome. *Dev. Biol.* 300:252–266. http://dx.doi.org/10.1016/j.ydbio.2006.07.044

Wickström, S.A., K. Radovanac, and R. Fässler. 2011. Genetic analyses of integrin signaling. *Cold Spring Harb. Perspect. Biol.* 3:a005116. http://dx.doi.org/10.1101/cshperspect.a005116

Worth, D.C., K. Hodivala-Dilke, S.D. Robinson, S.J. King, P.E. Morton, F.B. Gertler, M.J. Humphries, and M. Parsons. 2010. α v β3 integrin spatially regulates VASP and RIAM to control adhesion dynamics and migration. *J. Cell Biol.* 189:369–383. http://dx.doi.org/10.1083/jcb.200912014

Yang, J.T., B.L. Bader, J.A. Kreidberg, M. Ullman-Culleré, J.E. Trevithick, and R.O. Hynes. 1999. Overlapping and independent functions of fibronectin receptor integrins in early mesodermal development. *Dev. Biol.* 215:264–277. http://dx.doi.org/10.1006/dbio.1999.9451

Zaidel-Bar, R., C. Ballestrem, Z. Kam, and B. Geiger. 2003. Early molecular events in the assembly of matrix adhesions at the leading edge of migrating cells. *J. Cell Sci.* 116:4605–4613. http://dx.doi.org/10.1242/jcs.00792

Zaidel-Bar, R., S. Itzkovitz, A. Ma'ayan, R. Iyengar, and B. Geiger. 2007. Functional atlas of the integrin adhesome. *Nat. Cell Biol.* 9:858–867. http://dx.doi.org/10.1038/ncb0807-858

Zamir, E., M. Katz, Y. Posen, N. Erez, K.M. Yamada, B.Z. Katz, S. Lin, D.C. Lin, A. Bershadsky, Z. Kam, and B. Geiger. 2000. Dynamics and segregation of cell-matrix adhesions in cultured fibroblasts. *Nat. Cell Biol.* 2:191–196. http://dx.doi.org/10.1038/35008607

Zhang, X., G. Jiang, Y. Cai, S.J. Monkley, D.R. Critchley, and M.P. Sheetz. 2008. Talin depletion reveals independence of initial cell spreading from integrin activation and traction. *Nat. Cell Biol.* 10:1062–1068. http://dx.doi.org/10.1038/ncb1765

Zimmermann, J., D. Labudde, T. Jarchau, U. Walter, H. Oschkinat, and L.J. Ball. 2002. Relaxation, equilibrium oligomerization, and molecular symmetry of the VASP (336-380) EVH2 tetramer. *Biochemistry*. 41:11143–11151. http://dx.doi.org/10.1021/bi020379x